Int J Earth Sci (Geol Rundsch) (2013) 102:1627–1654
DOI 10.1007/s00531-013-0894-4

ORIGINAL PAPER

Modes of orogen-parallel stretching and extensional exhumation in response to microplate indentation and roll-back subduction (Tauern Window, Eastern Alps)

A. Scharf · M. R. Handy · S. Favaro · S. M. Schmid · A. Bertrand

Received: 15 October 2012 / Accepted: 21 March 2013 / Published online: 17 May 2013

Abstract The Tauern Window exposes a Paleogene nappe stack consisting of highly metamorphosed oceanic (Alpine Tethys) and continental (distal European margin) thrust sheets. In the eastern part of this window, this nappe stack (Eastern Tauern Subdome, ETD) is bounded by a Neogene system of shear (the Katschberg Shear Zone System, KSZS) that accommodated orogen-parallel stretching, orogen-normal shortening, and exhumation with respect to the structurally overlying Austroalpine units (Adriatic margin). The KSZS comprises a ≤5-km-thick belt of retrograde mylonite, the central segment of which is a southeast-dipping, low-angle extensional shear zone with a brittle overprint (Katschberg Normal Fault, KNF). At the northern and southern ends of this central segment, the KSZS loses its brittle overprint and swings around both corners of the ETD to become subvertical, dextral, and sinistral strike-slip faults. The latter represent stretching faults whose displacements decrease westward to near zero. The kinematic continuity of top-east to top-southeast ductile shearing along the central, low-angle extensional part of the KSZS with strike-slip shearing along its steep ends, combined with maximum tectonic omission of nappes of the ETD in the footwall of the KNF, indicates that north–south shortening, orogen-parallel stretching, and normal faulting were coeval. Stratigraphic and radiometric ages constrain exhumation of the folded nappe complex in the footwall of the KSZS to have begun at 23–21 Ma, leading to rapid cooling between 21 and 16 Ma. This exhumation involved a combination of tectonic unroofing by extensional shearing, upright folding, and erosional denudation. The contribution of tectonic unroofing is greatest along the central segment of the KSZS and decreases westward to the central part of the Tauern Window. The KSZS formed in response to the indentation of wedge-shaped blocks of semi-rigid Austroalpine basement located in front of the South-Alpine indenter that was part of the Adriatic microplate. Northward motion of this indenter along the sinistral Giudicarie Belt offsets the Periadriatic Fault and triggered rapid exhumation of orogenic crust within the entire Tauern Window. Exhumation involved strike-slip and normal faulting that accommodated about 100 km of orogen-parallel extension and was contemporaneous with about 30 km of orogen-perpendicular, north–south shortening of the ETD. Extension of the Pannonian Basin related to roll-back subduction in the Carpathians began at 20 Ma, but did not affect the Eastern Alps before about 17 Ma. The effect of this extension was to reduce the lateral resistance to eastward crustal flow away from the zone of greatest thickening in the Tauern Window area. Therefore, we propose that roll-back subduction temporarily enhanced rather than triggered exhumation and orogen-parallel motion in the Eastern Alps. Lateral extrusion and orogen-parallel extension in the Eastern Alps have continued from 12 to 10 Ma to the present and are driven by northward push of Adria.

Keywords Tauern Window · Katschberg Shear Zone System · Stretching fault · Indentation · Roll-back subduction · Lateral extrusion

A. Scharf (✉) · M. R. Handy · S. Favaro · S. M. Schmid · A. Bertrand
Department of Earth Sciences, Freie Universität Berlin, Malteserstrasse 74-100, 12249 Berlin, Germany
e-mail: scharfa@zedat.fu-berlin.de

S. M. Schmid
Department of Geophysics, Eidgenössische Technische Hochschule (ETH), Sonneggstrasse 5, 8092 Zurich, Switzerland

A. Bertrand
alps GmbH, Center for Climate Change and Adaptation Technologies, Grabenweg 68, 6020 Innsbruck, Austria

Introduction

Understanding how Alpine-type mountain belts grow is an elusive endeavor owing to their highly arcuate and non-cylindrical structure. Controversy centers on the relative contributions of shortening, extension, and erosion to this growth, as discussed, for example, for the Alps-Carpathian segment of the Adria-Europe collision zone (inset to Fig. 1; e.g., Royden and Burchfield 1989; Selverstone 2005) and the India-Asia collision zone (e.g., Johnson 2002). In the latter case, lithospheric thickening due to thrusting and folding accommodated only 40–50 % of the collisional plate convergence, with most of this shortfall accommodated by lateral motion of upper-plate lithosphere away from the zone of plate indentation (e.g., Tapponnier et al. 1986; Royden et al. 1997) and/or by erosion, e.g., along the accretionary front of the Himalayan Orogen (e.g., Beaumont et al. 2001).

The eastern part of the Alps with its core of exhumed Cenozoic basement nappes in the Tauern Window (Fig. 1) is part of a three-dimensional kinematic system where orogenic crust and lithosphere (AlCaPa Unit in inset of Fig. 1) thin eastward over a distance of only 200 km, from maximum values of 50 and 220 km, respectively, in the Eastern Alps to 25 and 60 km, respectively, in the Miocene Pannonian Basin (Praus et al. 1990; Horváth 1993; Lenkey 1999; Waldhauser et al. 2002; Horváth et al. 2006 and references therein; Kissling et al. 2006). This orogen-parallel reduction in thickness of crust and lithosphere is linked to syn-orogenic extension and basin formation within the AlCaPa and Tisza units during roll-back subduction beneath the Carpathians (Fig. 1; Ustaszewski et al. 2008). This raises the issue of whether eastward, lateral extrusion of thickened orogenic crust was caused by "push" of the impinging Adriatic microplate (Ratschbacher et al. 1991b; Rosenberg et al. 2007), or alternatively, by "pull" of the eastwardly retreating European subduction slab beneath the Carpathians (Fodor et al. 1999), or by some combination of these two forces. A related debate concerns whether north–south shortening during Adria-Europe convergence was accommodated primarily by upright folding and erosion with only modest east–west orogen-parallel extension (e.g., Laubscher 1988; Rosenberg et al. 2007) or by conjugate strike-slip faulting and low-angle normal faulting toward the Pannonian Basin (Ratschbacher et al. 1989, 1991b; Frisch et al. 1998; Linzer et al. 2002).

The Tauern Window holds key information to resolve these questions. Its topographic relief of more than 3,000 m provides excellent three-dimensional exposure of large-scale folds, shear zones, and faults (Fig. 1) that substantially modified the Paleogene nappe stack formed during south-directed subduction of the Mesozoic Alpine Tethys Ocean and distal parts of the European margin. The Subpenninic–Penninic nappe stack derived from this lower plate is the same as that exposed in the Western Alps and found to the east in boreholes and/or imaged seismically beneath the northern part of the Pannonian Basin (Schmid et al. 2008). In contrast, the overlying Austroalpine nappes that frame the Tauern Window are derived from the continental margin of the Adriatic upper plate and can also be traced eastward to the subsurface of the Pannonian Basin. These nappes formed at an earlier stage of Adria-Europe convergence, i.e., during Late Cretaceous orogeny (e.g., Froitzheim et al. 2008; Handy et al. 2010), so their subdivision is not pertinent to our study of Neogene lateral extrusion. Following Ratschbacher et al. (1991b), we use the term lateral extrusion to refer to a combination of conjugate strike-slip faulting ("lateral escape", Tapponnier et al. 1986), low-angle normal faulting ("lateral extension", Dewey et al. 1988), and lower crustal flow (Royden et al. 1997) which, acting alone or in concert, move orogenic lithosphere at high angles to the convergence vector and subparallel to the orogen.

In this paper, we present new structural data showing that lateral extrusion of accreted European basement nappes, Alpine Tethyan units and the lowermost Austroalpine nappes in the Tauern Window was triggered by Neogene northward indentation of Adriatic lithosphere. After a brief introduction to the geology in the eastern part of the Tauern Window ("Tectonic setting" section), we describe a kinematically linked system of low-angle normal fault, strike-slip faults, and domes that allowed the Alpine orogenic edifice to expand some 20–30 km to the ESE while undergoing north–south shortening ("Katschberg Shear Zone System" section). We then use available petrological and thermochronological data to constrain the exhumation history of the deformed nappe stack during lateral extrusion ("Metamorphic conditions in the Eastern Tauern Subdome and the timing of Katschberg-related deformation" section). We show that stretching and normal faulting ("Strain partitioning between folding, normal faulting and strike-slip faulting in the Eastern Tauern Window" section) are integral to the process of eastward lateral extrusion in the Eastern Alps ("Relationship of lateral extrusion to Adria-Europe convergence" section). We conclude by comparing the importance of Adria indentation and Carpathian slab retreat in driving lateral orogenic escape ("Implications for the forces driving lateral extrusion" section).

Tectonic setting

The Tauern Window exposes Penninic and Subpenninic nappes that accreted with units of the distal European

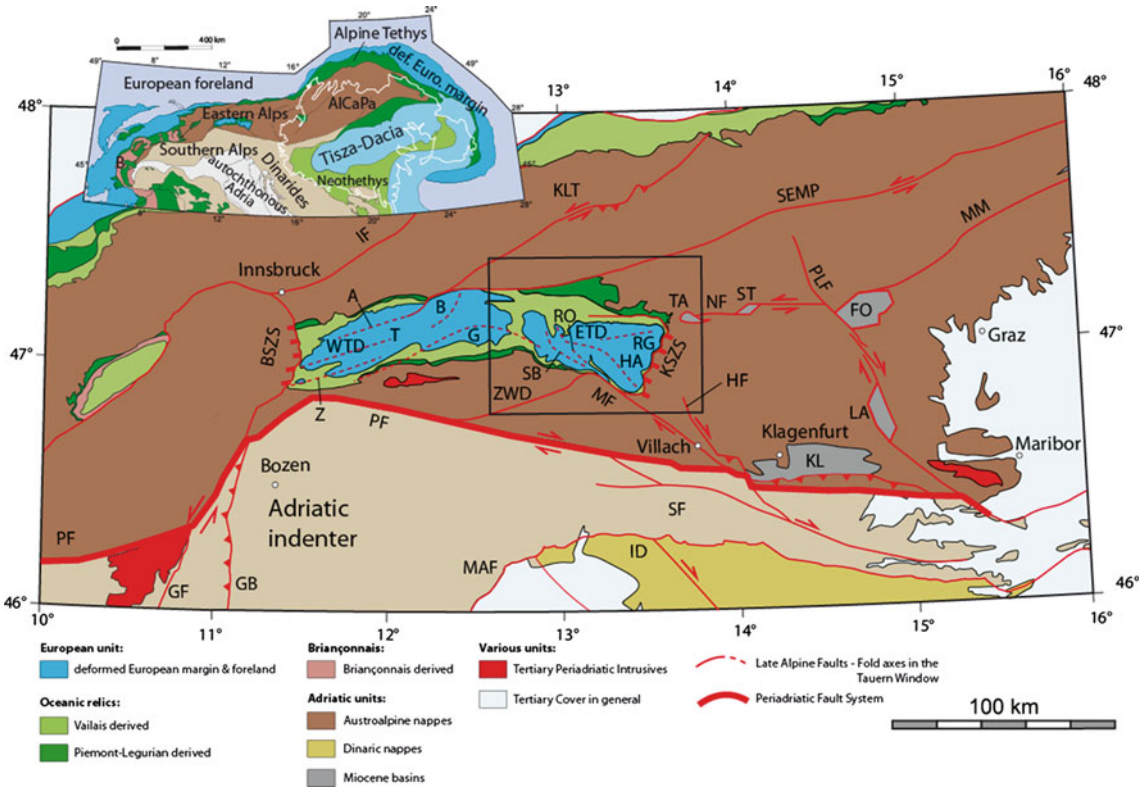

Fig. 1 Tectonic map of the Eastern Alps, with *box* showing study area. Faults and shear zones: *BSZS* Brenner Shear Zone System, *HF* Hochstuhl Fault, *GF* Giudicarie Fault, *IF* Inntal Fault, *KLT* Königsee-Lammertal-Traunsee Fault, *KSZS* Katschberg Shear Zone System, *ID* Idrija Fault, *MF* Mölltal Fault, *MM* Mur-Mürz Fault, *NF* Niedere Tauern Southern Fault, *MT* Maniago Thrust, *PF* Periadriatic Fault, *PLF* Pöls-Lavantal Fault System, *SEMP* Salzach-Ennstal-Mariazell-Puchberg Fault, *SF* Sava Fault, *ZWD* Zwischenbergen-Wöllatratten-Drau Fault. Fold and thrust-belt: *GB* sinisitrally transpressive Giudicarie Belt. Fold axes within the Tauern Window: *A* Ahorn, *B* Breitfuss, *G* Granatspitz, *HA* Hochalm, *RG* Rotgülden, *RO* Romate, *SB* Sonnblick, *T* Tux, *Z* Zillertal. Neogene basins: *FO* Fohnsdorf, *KL* Klagenfurt, *LA* Lavanttal, *ST* Seetal, *TA* Tamsweg; *ETD* Eastern Tauern Subdome, *WTD* Western Tauern Subdome. *Inset* map shows major units of Alps and Carpathians and the major tectonic plates (Europe, Adria), *B* Briançonnais. *White line* delimits the Pannonian Basin. Maps modified from Nussbaum (2000), Schmid et al. (2004, 2008, in press), Wölfler et al. (2011)

continental margin during Paleogene imbrication of Alpine Tethyan oceanic units (Matrei Zone, Glockner Nappe System: e.g., Kurz et al. 1998, 2008; Schmid et al., in press; Fig. 2). Two basement subdomes at either end of the Tauern Window expose these continental units in duplex structures that formed at around 30 Ma ago (Fig. 1, Eastern and Western Tauern subdomes). These duplex structures characterize the Venediger Nappe System (Lammerer and Weger 1998; Schmid et al., in press) which were subsequently deformed by upright, doubly plunging folds. This folded nappe system is bounded at both ends by low-angle extensional shear zones, the Brenner- and Katschberg normal faults. These are kinematically linked to conjugate strike-slip shear zones to form what we refer to as the Brenner- and Katschberg shear zone systems (BSZS and KSZS; Fig. 1). Both systems separate the Cenozoic metamorphic units in the Tauern Window from the overlying Late Cretaceous Austroalpine nappes (Fig. 1). Here, we focus on the kinematics of folding and shearing within the Eastern Tauern Subdome, in particular along the Katschberg Shear Zone System.

Katschberg Shear Zone System

Ductile shearing in the Katschberg Shear Zone System

Genser and Neubauer (1989) first described a normal fault at the eastern end of the Eastern Tauern Subdome, which they referred to as the Katschberg Normal Fault (KNF). At first glance, the KNF appears to be a classical low-angle normal fault comprising a 30–45° southeast-dipping mylonitic shear zone capped to the east by a brittle normal fault. This fault exhumed Penninic units in its footwall parallel to a southeast-plunging stretching lineation. However, our mapping revealed that the mylonites in the

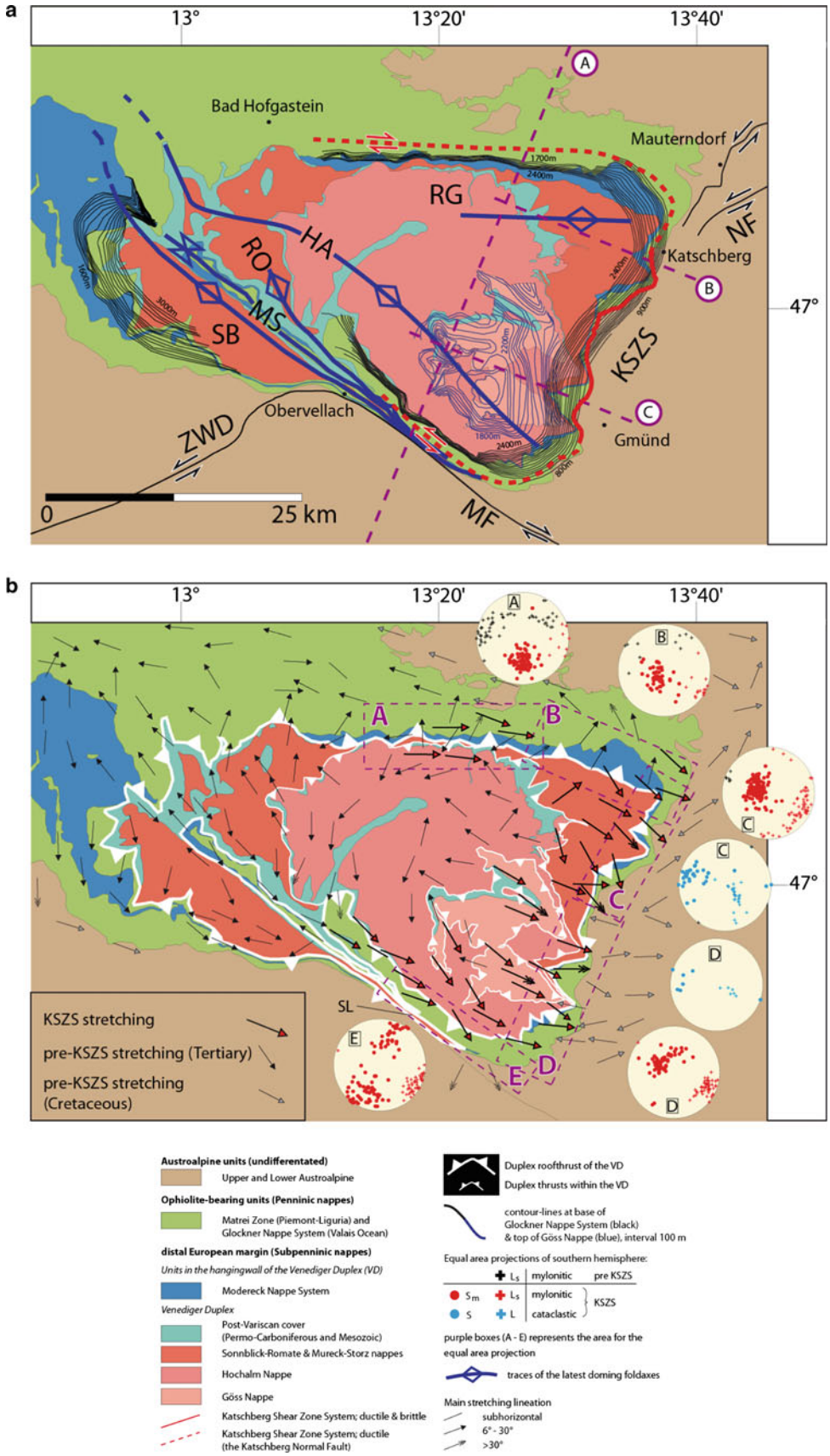

Fig. 2 Structure of the Eastern Tauern Subdome: **a** Contours: *black*—basal thrust of the Glockner Nappe System, *blue*—top of the Göss Nappe in the Venediger Nappe System; Post-nappe folds and dome axes: *HA* Hochalm Dome, *RG* Rotgülden Dome, *RO* Romate Fold, *SB* Sonnblick Dome, *MS* Mallnitz Synform. Brittle Faults: *MF* Mölltal Fault, *NF* Niedere Tauern Southern Fault, *ZWD* Zwischenbergen-Wöllatratten-Drau Fault. *Purple dashed lines* show traces of cross-sections in Fig. 3; **b** Stretching lineations, Ls compiled from own measurements and Becker (1993), Exner (1956, 1962a, 1980, 1983, 1989), Frank (1965). *Equal-area plots* show orientations of Sm (*dots*) and Ls (*crosses*) of the fabric domains A–E (own measurements). *SL* Sonnblick Lamellae. Tectonic map simplified from Schmid et al. (in press)

footwall of the KNF only represent the central part of a much larger and thicker belt of ductile shearing that envelops the entire eastern perimeter of the Tauern Window (Fig. 2). We refer to this arcuate mylonitic belt, including brittle overprint along the KNF, as the Katschberg Shear Zone System (KSZS). We emphasize, however, that only the central, normal-fault segment, i.e., the KNF, is capped by cataclasites. The KSZS deforms the underlying Venediger Nappe System, particularly in the vicinity of the major thrust at the base of the Austroalpine nappes which emplaced these nappes onto the Penninic and Subpenninic units in Paleogene time (Fig. 1). The KSZS is therefore a late-orogenic feature that post-dates structures dating from Latest Cretaceous to Paleogene subduction, accretion, collision, and nappe stacking.

The KNF comprises a wide (≤5 km thick) belt of retrograde amphibolite- to greenschist-facies mylonite (Fig. 3b, c) that affects primarily calc-schist of the Penninic oceanic units as well as a broad zone in underlying Variscan gneisses of the Subpenninic basement and cover sequences. As shown in Fig. 2, this ductile shear zone swings continuously around the Eastern Tauern Subdome and connects with two subvertical shear zones that carry subhorizontal stretching lineations: a northern dextral shear zone that strikes east–west and ends near Bad Hofgastein, and a southern sinistral shear zone that trends WNW–ESE, parallel to the dextral and brittle Mölltal Fault (Fig. 2a). The cataclasites capping the KNF gradually disappear toward the arcuate parts of the KSZS where the KNF swings into the subvertical shear zones (Fig. 2a). Near the termination of the northern branch at Bad Hofgastein, the steep mylonitic foliation gradually becomes indistinguishable from older Alpine foliations and loses its subhorizontal stretching lineation. The southern branch of the KSZS ends in the vicinity of Obervellach (Fig. 2a). Northwest of this locality, the sinistral southern branch of the KSZS broadens, subhorizontal lineations become rare, and the shear zone grades into a series of km-scale folds (Romate Antiform, Mallnitz Synform and Sonnblick Antiform; Fig. 2a). Yet further to the northwest, these folds become open and eventually die out. The Mallnitz Synform, for example, extends all the way to the western end of the Sonnblick Dome before acquiring a northwest trend and losing its amplitude entirely (Exner 1964). All these transitions document a kinematic link, and hence, contemporaneity of dextral and sinistral shearing along the northern and southern branches of the KSZS during north–south shortening.

The low-angle, central segment of the KSZS (the KNF, Genser and Neubauer 1989) is characterized by mylonites with a foliation that dips 25–30° to the E to SE and carries a down-dip stretching lineation. This mylonitic foliation overprints variably oriented pre-Alpine and Paleogene schistosities in the Subpenninic and Penninic units, as well as a Late Cretaceous schistosity in the Katschberg Quartzphyllite Unit forming the base of the Austroalpine units (Fig. 2b).

Km-scale upright folds (axial traces in Fig. 2a) deform the duplex structure of the Venediger Nappe System in the footwall of the KSZS. Upright folding of an antiformal stack was first observed in the Western Tauern Subdome (Lammerer and Weger 1998), where the amplitude of the folds is much larger than in the Eastern Tauern Subdome and where the axial planes trend subparallel to the strike of the thrust sheets within the duplex (Fig. 1). In the Eastern Tauern Subdome, the angle between duplex-related structures and the NW–SE and WSW–ENE striking fold axes (Hochalm, Rotgülden, respectively) is greater, yielding complex interference patterns in map view. Note that the southeastern lobe of the Eastern Tauern Subdome mimics the shape of the southeast-plunging Hochalm Antiform (Fig. 2a); this is also where the KNF shows the greatest amount of tectonic omission in its footwall (area D in Fig. 2b). These features support the idea that north–south shortening is not only contemporaneous with dextral and sinistral shearing along northern and southern branches of the KSZS, but also with top-SE extensional shearing across the KNF.

The stretching lineation on the mylonitic foliation of the KSZS trends ESE–WNW and plunges to the ESE, irrespective of the orientation of this foliation around the Eastern Tauern Subdome. A host of kinematic indicators (Fig. 4) confirms that sense of shear is top-E to top-SE along the KNF (Fig. 4a, b), dextral in map view along the steep to moderately dipping northern branch of the KSZS (Fig. 4c) and sinistral along the subvertical southern branch (Fig. 4d). The scatter in the orientation of the lineation in fabric domains A, B, and C (Fig. 2b) can be attributed to a strong coaxial component of mylonitic shearing and/or to the local preservation of older mylonitic fabrics related to nappe stacking. A component of coaxial shearing is recorded by *c*-axis textures of dynamically recrystallized quartz and calcite aggregates in the Sonnblick Dome and Sonnblick Lamellae (Kurz and Neubauer 1996). Near the western terminations of the KSZS, kinematic indicators become rare or are equivocal, with both dextral and sinistral shear senses recorded.

We emphasize that our determination of a sinistral shear sense along the southern branch of the KSZS, including the Sonnblick Gneiss Lamellae, is a radical departure from previous interpretations in which shearing parallel to the NW–SE striking southeastern margin of the Tauern Window was predominantly dextral (e.g., Kurz and Neubauer 1996). The observed sinistral shear sense along this southern branch is a key to its interpretation as stretching faults ("Coeval folding, normal faulting and stretching"

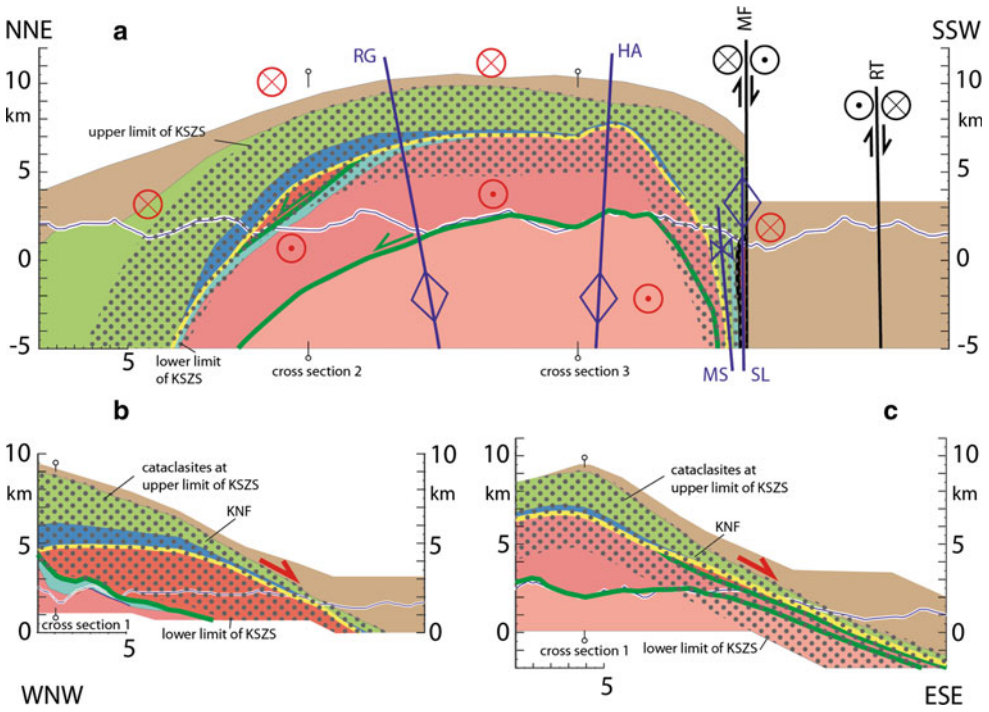

Fig. 3 Cross-sections across the easternmost Tauern Window along profile traces shown in Fig. 2a: **a** section normal to the Katschberg transport direction showing the northern and southern branches of the KSZS straddling the Hochalm (HA) and Rotgülden (RG) domes that shorten the underlying Venediger Nappe System. Other structures include the Mallnitz Synform (MS), Sonnblick Gneiss Lamellae (SL), Mölltal Fault (MF), and the Ragga-Teuchl Fault (RT); **b**, **c** cross-sections parallel to the ESE-directed transport direction of the KSZS and perpendicular to the KNF, respectively. *Gray stippled pattern* indicates mylonitic Katschberg shearing; the mylonite belt is capped by cataclasites. *Green lines* are nappe contacts within the Venediger Nappe System; the *yellow line* outlines the roof thrust. Major nappe contacts and fault boundaries were constructed with the aid of structural contour maps

section). Note that the Mölltal Fault, immediately adjacent to and south of the mylonites of the KSZS, is indeed dextral as claimed by Kurz and Neubauer (1996). However, this fault is entirely brittle ("Brittle faulting" section).

Brittle faulting

The brittle lid of the KNF consists of a zone of cataclasites underlain by a 10–100-m-wide zone with closely spaced, semi-brittle (discrete) shear zones that overprint mylonites of the KNF. Semi-brittle shearing below the cataclasites is associated with small-scale drag of the older mylonitic foliation, which it overprints in kinematic continuity (Fig. 4b; Genser and Neubauer 1989; their Fig. 2d). The discrete shear bands dip c. 45° to the southeast, parallel to the cataclasites of the KNF. Rocks within the semi-brittle shear zone contain retrograde white mica and chlorite indicative of lower greenschist-facies conditions during shearing. Both the mylonites and the discrete shear bands indicate top-E to top-SE displacement of the Austroalpine units in the hanging wall (Genser and Neubauer 1989). Identical kinematics and similar mineralogy indicating synkinematic retrogression of fabrics at the top of the KNF suggest that brittle shearing was continuous with and outlasted mylonitic shearing.

We emphasize that the brittle lid of the KNF is restricted to the central, normal-fault segment of the KSZS and that we were unable to map a northern or southern continuation of these cataclasites along the KSZS. As mentioned above, tectonic omission of the footwall of the KNF reaches a maximum where it exhumes the Hochalm Dome in its footwall, strengthening our interpretation that Katschberg shearing and faulting were coeval with doming and upright folding. Brittle faulting is also known from the "Niedere Tauern Southern Fault" (NF in Fig. 1; Eder and Neubauer 2000; Reinecker 2000; Wölfler et al. 2011; Schmid et al., in press). However, we were unable to map a continuous zone of cataclasites connecting the KNF and the NF in this poorly exposed area. Such a connection is not expected anyway, because the NF bounds several pull-apart basins located within the hanging wall of the KNF rather than at its base. The sedimentary fill of these basins postdates much of the activity of the KNF and serves to constrain the age of late

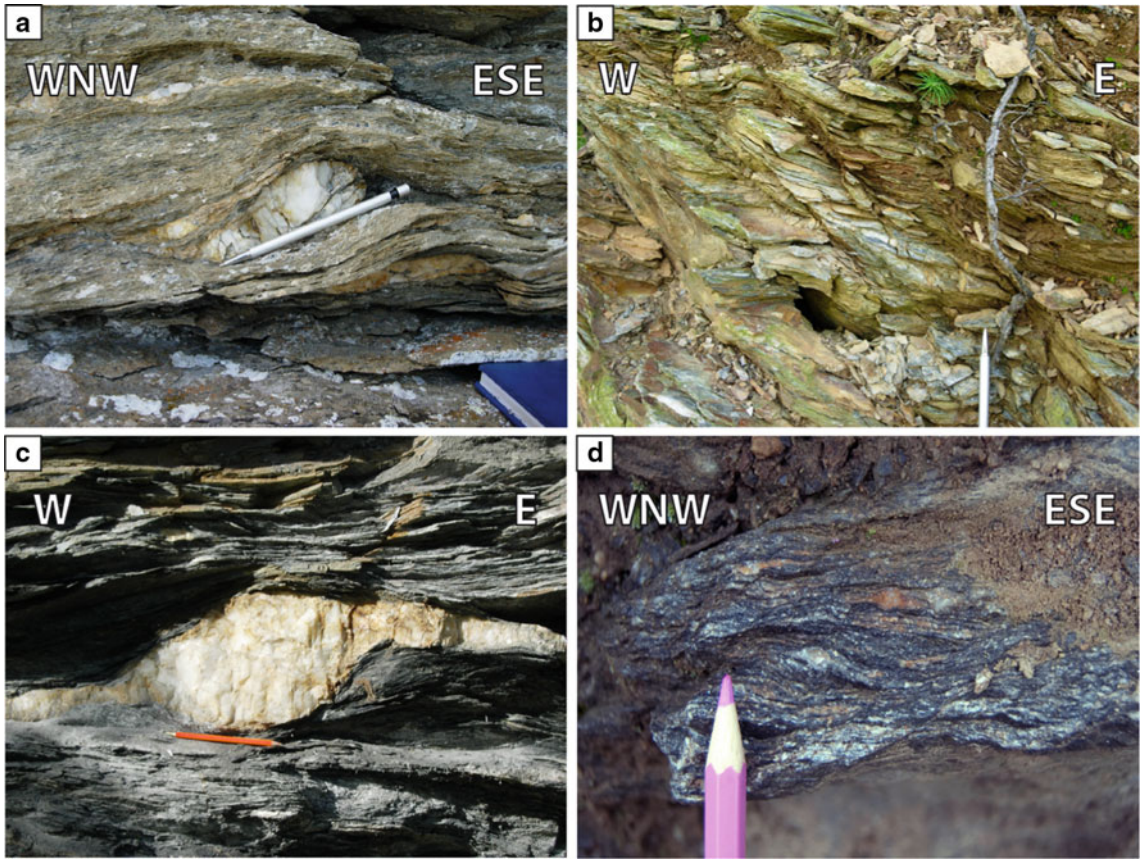

Fig. 4 Structures of the Katschberg Shear Zone System: **a** rotated quartz clast indicating top-ESE shear sense in calc-schist of the Glockner Nappe System along the KNF (N 47°01′11.1″ E 13°32′26.9″, elevation 2,469 m); **b** semi-brittle discrete shear planes overprinting mylonites of the KNF derived from the Austroalpine Katschberg Quartzphyllite located a few tens of meters below the brittle lid of the KNF (N 47°02′13.9″ E 13°35′54.5″, elevation 1,491 m); **c** sigma clast indicating dextral shear sense along the northern branch of the KSZS in calc-schist of the Glockner Nappe System (upper Muhr Valley, N 47°08′46.1″ E 13°23′06.2″, elevation 1,722 m); **d** sinistral shear bands along the southern branch of the KSZS in the Sonnblick orthogneiss from the southeastern tip of the Sonnblick Lamellae (Möll Valley, N 46°53′17″ E 13°18′19.1″ 800 m)

stages of the lateral extrusion in the Austroalpine units ("Timing constraints" section).

The brittle dextral Mölltal Fault only affects Austroalpine basement rocks located immediately to the south, hence, in the hanging wall of the KSZS. Cataclasites are beautifully exposed in outcrops along the new southern ramp of the Tauern Railroad (e.g., village of Pusarnitz, 20 km to the ESE of Obervellach in Fig. 2a, N 46°50′42.2″ E 13°22′49.5″). There, the kinematics and crosscutting relationships of shear surfaces indicate conjugate strike-slip motion sub-parallel to the Mölltal Fault, followed by SW-down normal faulting.

The Mölltal Fault locally overprints the sinistral southern mylonitic branch of the KSZS that is best exposed north of the Mölltal Fault along the steep northern side of the Möll Valley. This indicates that brittle dextral motion on the Mölltal Fault syn- to post-dated sinistral mylonitic shearing along the southern branch of the KSZS. We found no evidence for the continuation of the Mölltal Fault into the Mallnitz Synform, as previously reported (Kurz and Neubauer 1996; Wölfler et al. 2011). We are aware of the fact that local occurrences of cataclasites have been described parallel to the hinge zone of the Sonnblick Antiform (Riedmüller and Schwaighofer 1970, 1971) and that these partly coincide with a minor step in low-temperature thermochronometric ages (zircon (U-Th)/He, apatite fission track, apatite (U-Th/He) in Wölfler et al. 2012). However, the strains achieved at these locations are minor, and these cataclasites are spatially and, hence, kinematically unrelated to strike-slip faulting along the Mölltal Fault. Instead, the northwestern end of the Mölltal Fault broadens into a diffuse zone of cataclasites near Obervellach (Fig. 2a) that skirts, but does not enter the Sonnblick Dome. We suspect that this is where the Mölltal Fault conjoins with the conjugate Zwischenbergen-Wöllatratten-Drautal (ZWD) Fault (Figs. 1, 2a). These two strike-slip faults are interpreted to

bound a wedge-shaped piece of Austroalpine basement, which we will refer to as the "Drau-Möll Block" (see "Faults in the Austroalpine basement and their bearing on indentation of the Eastern Tauern Subdome" section). Note that further to the southeast, the Mölltal Fault does not link with the KSZS either (Fig. 2). Whereas the KSZS swings around to form the KNF, the Mölltal Fault continues straight to the southeast where it is covered by Plio-Pleistocene deposits of the Drau Valley before merging with, and slightly offsetting, the Periadriatic Fault (Fig. 1; Bigi et al. 1989). The dextral Hochstuhl Fault (Fig. 1) is yet another young (post-Sarmatian to recent) dextral Riedel Fault that also offsets the Periadriatic Fault and delimits Late Neogene-to-Recent North Karawanken dextral transpressive overprint of the Periadriatic Fault to the west (Polinski and Eisbacher 1992; Vrabec and Fodor 2006).

Displacement along the KSZS

We calculated a maximum throw of 13.5 km across the southern part of the central low-angle segment of the KSZS by comparing the geometry and thickness of Penninic and Subpenninic nappes where their tectonic omission is greatest (near Gmünd in Fig. 2, cross-sections in Fig. 3b, c) with those of the same nappe contacts away from the KSZS (Schmid et al., in press; their cross-sections 7–10 in Fig. 3). There, the deepest Subpenninic unit (Göss Nappe) in the footwall is juxtaposed in map view with the lowest Austroalpine unit in the hanging wall. Given the current 25–30° dip of the mylonites of the KNF in this area, the throw of 13.5 km corresponds to a heave (horizontal displacement) of 23–29 km. Obviously, the displacement may exceed 29 km if the dip of the KSZS at the time of shearing was less than that presently observed; doming of the hot Penninic units during Katschberg shearing may have steepened the KSZS during the late stages of extensional shearing. In fact, apatite Fission Track (AFT) and (U-Th)/He ages along a north–south transect of the Hochalm Dome indicate that the cooling rate of 9–12 °C/Ma has increased since 6 Ma (Foeken et al. 2007) and leveling surveys along the Tauern railroad tunnel reveal ongoing uplift at 1–2 mm/a in the core of the Hochalm Dome below the Katschberg Normal Fault (Senftl and Exner 1973). Taken together, this suggests that the eastern margin of the KSZS has steepened during the later stages of its evolution and indeed continues to steepen today.

Our estimates of displacement on the KNF are comparable to those of Genser and Neubauer (1989) who calculated a throw of 10 km from the difference in the peak temperatures of Alpine metamorphism in the hanging wall (Austroalpine units at 300 °C) and footwall (Göss Nappe at 600 °C) for an assumed syntectonic geothermal gradient of 30 °C/km (Grundmann and Morteani 1985). This gradient must be regarded as an absolute minimum value in light of data indicating a transient, syntectonic gradient of as much as 70 °C/km across the KSZS (Scharf 2013). Most of the displacement must have been taken up by the mylonites of the KNF as it is only the mylonites that bend around the eastern margin of the Tauern Window into the strike-slip segments of the KSZS. The horizontal offset along these segments at the points of greatest curvature of the KSZS in map view must be equivalent to the heave (minimum 23–29 km) on the central, low-angle part of the KSZS. However, in view of the westward termination of the KSZS discussed above, offset gradually decreased westward, as expected for stretching faults ("Coeval folding, normal faulting and stretching" section).

Metamorphic conditions in the Eastern Tauern Subdome and the timing of Katschberg-related deformation

Pressure and temperature conditions

Figure 5 shows the distribution of isograds and isotemperature contours related to the thermal peak of metamorphism, the so-called "Tauernkristallisation" (Sander 1911), an amphibolite-facies event in the eastern and western subdomes of the Tauern Window at around 30–28 Ma (Rb/Sr on garnet-bearing assemblages, Christensen et al. 1994; Rb/Sr white mica of von Blanckenburg et al. 1989; Kurz et al. 2008; U–Pb allanite, Cliff et al. 1998; Inger and Cliff 1994). The concentric isotemperature contours in Fig. 5 cut across nappe contacts below the KSZS and coincide with the culmination of the Hochalm Dome, where peak conditions of 630 ± 40 °C (Cliff et al. 1985; Droop 1985; Scharf 2013) and 0.76 ± 0.12 GPa (Cliff et al. 1985; Droop 1985) indicate a total exhumation of 25 km.

Syntectonic metamorphism in the KSZS decreases from amphibolite-facies along its base in the Subpenninic units to lower greenschist-facies in mylonite just below the brittle top of the KNF (stippled domains in Figs. 3, 6a). This shearing occurred during and/or after the attainment of peak temperatures in the Eastern Tauern Subdome as indicated by the closer spacing of the 500° and 550 °C contours in areas of tectonic omission along the central, low-angle part of the KSZS (Fig. 5). We attribute this to thinning of the previously equilibrated isotherms during Katschberg shearing under retrograde conditions. The narrow spacing of the 500° and 550 °C isotemperature contours along the southern branch of the KSZS and in the Mallnitz Synform is likewise attributed to mylonitic thinning and related post-nappe folding.

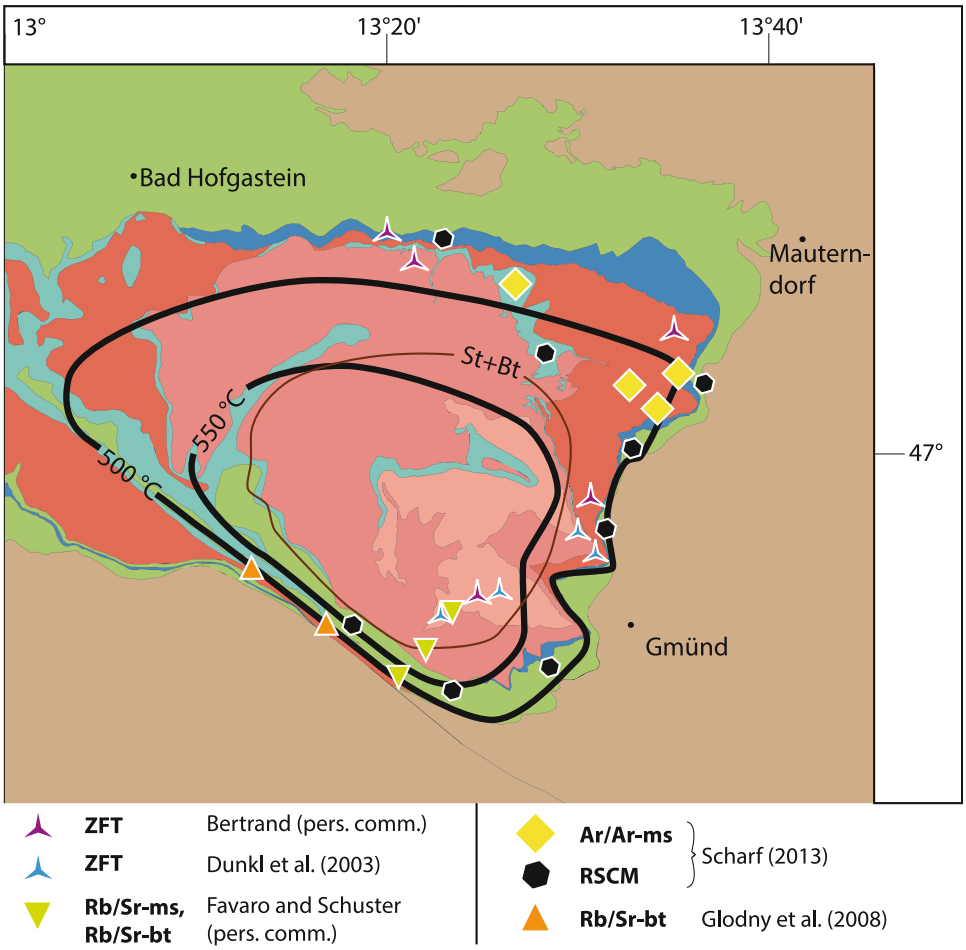

Fig. 5 Alpine metamorphism and sample locations for thermochronology in the Katschberg Shear Zone in the Eastern Tauern Subdome. The staurolite + biotite (St + Bt) isograde from Droop (1981, 1985) and the iso-cooling temperature contours for the Rb/Sr and K/Ar biotite systems compiled in Handy and Oberhänsli (2004, and references therein). Note that the T_{max} contours and the St + Bt isograde cut the nappe contacts. *Symbols* show localities of samples used in Fig. 7. *ZFT* zircon fission track, *RSCM* Raman microspectroscopy on carbonaceous material, Legend for tectonic units as in Fig. 2

Mylonitic gneisses from the KNF show different mechanisms of dynamic recrystallization in quartz (Fig. 6a). The fabric transition downward from the base of the KNF to the underlying Venediger Nappe System is gradational and marked by late-stage static recrystallization of quartz and albite aggregates (Fig. 6b) under amphibolite-facies conditions. Higher up within the mylonites of the KNF, quartz grains have arcuate and lobate grain boundaries that are indicative of fast grain boundary migration recrystallization (Fig. 6c; Stipp et al. 2002, 2004). However, annealed quartz structures are still preserved between microlithons of these mylonites (Fig. 6d).

Within the mylonites near the brittle top of the KNF, progressive subgrain rotation becomes the dominant mode of dynamic recrystallization in quartz (Fig. 6e) and is in turn replaced by bulging recrystallization immediately beneath the cataclasites of the KNF. Micaceous mylonite in calc-schist of the Glockner Nappe System typically contains shear bands indicative of top-E motion (Fig. 6f). Taken together, these quartz microstructures are interpreted to reflect a syntectonic thermal gradient characterized by a temperature of at least 500 °C at the base of the KNF to about 300–270 °C (Stipp et al. 2002, their Fig. 5) along its top, where the mylonites are cataclastically overprinted.

Constraints on the ages of exhumation of Tauern subdomes and activity of the KSZS

Temperature–time data for both the Katschberg- and Brenner shear zone systems in the Eastern and Western Tauern subdomes, respectively, are compiled in Fig. 7 from published data and new thermochronological work. Note that we do not discuss the thermal evolution related to Late Cretaceous to Early Cenozoic subduction, nappe stacking, and early exhumation (Ratschbacher et al. 2004; Kurz et al. 2008 and references therein), but instead focus on the post-collisional exhumation of the nappe stack after the thermal peak of metamorphism at 30–28 Ma (Selverstone et al. 1995), the so-called "Tauernkristallisation", that affected Subpenninic and Penninic units in the Tauern Window as described above. To allow a meaningful comparison of samples and systems similarly affected by deformation and exhumation along the margins of the Tauern Window, we constructed the temperature–time

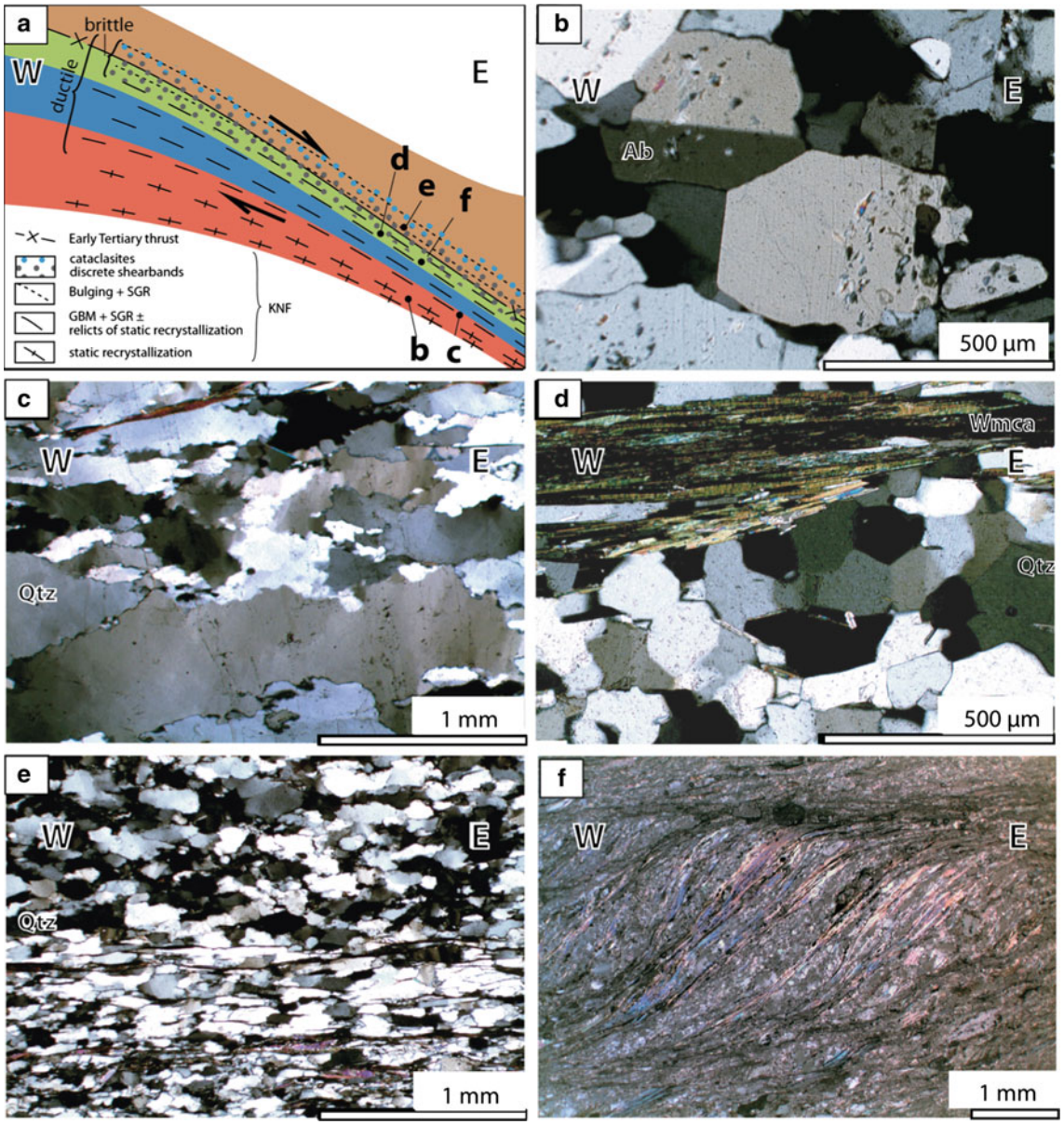

Fig. 6 Microstructures of the KSZS: **a** cross-section of the KNF with sample locations for **b**–**f**. Quartz fabric domains: *SGR* subgrain rotation, *GBM* grain boundary migration. Note that fabric domains overprint nappe boundaries. Legend for tectonic nappes as in Fig. 2; **b** static recrystallization and 120° triple junctions in albite aggregates at the base of the KSZS some 3 km below the brittle top of the KNF (sample AS 100: N 47°08′19.4″ E 13°33′46.6″, elevation 2,284 m); **c** fast migration in quartz aggregates from high-temperature mylonite of the KNF (sample AS101: N 47°08′15.4″ E 13°34′02.6″ 2,249 m; **d** statically recrystallized quartz in upper greenschist-facies KNF mylonite along the central/upper part about 1 km below the top of the KNF (sample AS1: N 47°03′14.4″ E 13°35′12.7″, elevation 1,959 m); **e** dynamically recrystallized quartz in greenschist-facies mylonite toward the top of the KNF (sample AS43: N 47°02′13.9″ E 13°35′54.5″ 1,491 m); **f** S–C fabric indicating top-E sense of shear in calc-schist (Glockner Nappe System) located 2 km below the top of the KNF (sample AS38: N 47°00′58.5″ E 13°32′36.9″, elevation 2,219 m). All photos were taken with crossed nichols. Mineral abbreviations from Siivola and Schmid (2007)

diagram in Fig. 7 using only samples from within the Katschberg- and Brenner shear zones systems (for details see Fig. 5, caption to Fig. 7). Samples from localities structurally above and below these shear zones were not included (all locations and used data compiled from the literature shown in "Appendix", Fig. 12; Table 1).

Figure 7 reveals a wide spread of ages especially for the $^{40}Ar/^{39}Ar$ white mica and zircon fission track systems in the KSZS (discussion below). For this reason, we have drawn swaths rather than lines through the weighted mean of the ages in the system brackets to illustrate the cooling trends in the eastern and western parts of the Tauern

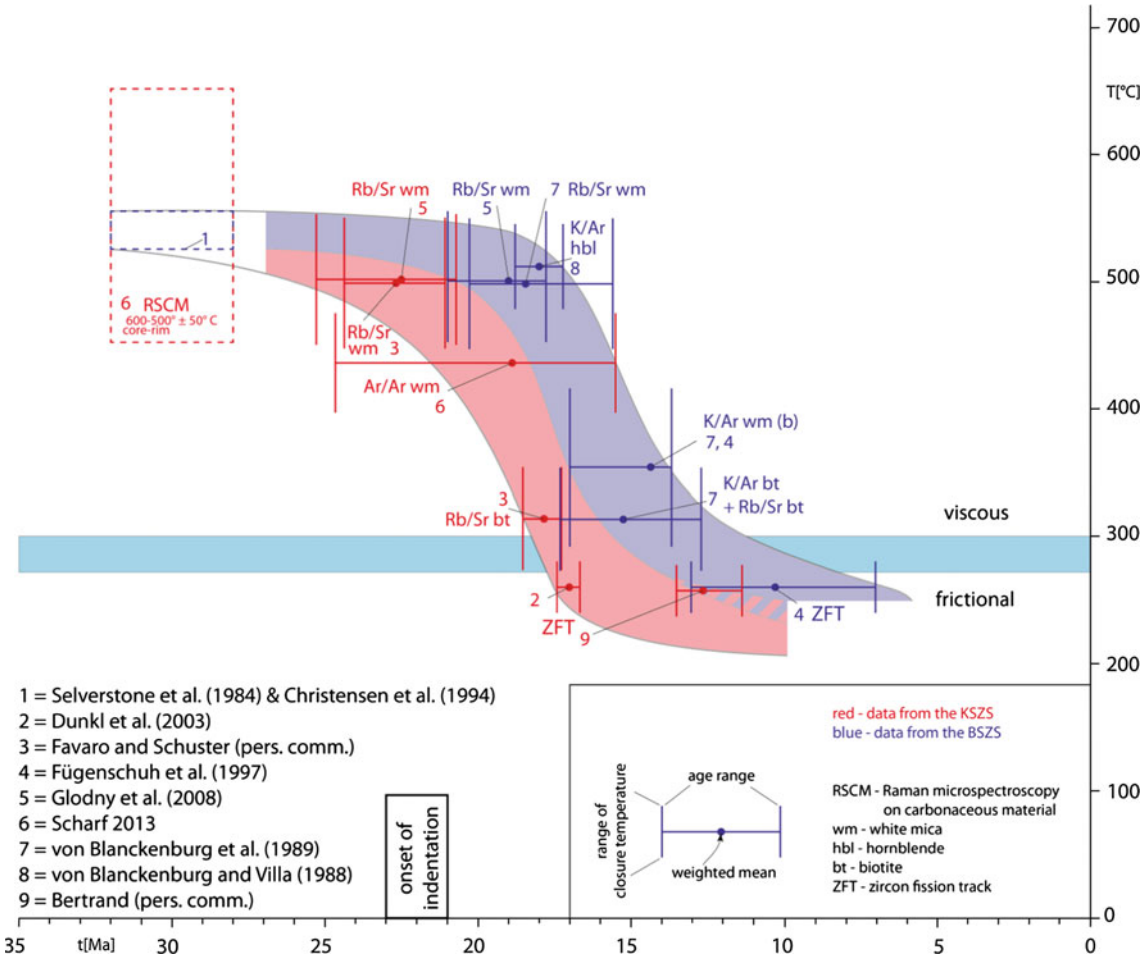

Fig. 7 Temperature-time evolutions of the Katschberg- and Brenner shear zone systems (KSZS and BSZS) derived from samples within the mylonites. *Blue symbols* apply to the BSZS, *red symbols* to the KSZS, see legend at *lower right* corner for explanation of the brackets and numbers for each age system. All samples, systems, and localities are listed in the "Appendix" (Fig. 12; Table 1). Temperature interval of frictional-viscous transition in quartz-rich rocks taken from Handy et al. (1999) and Stipp et al. (2002). *Dashed boxes* at *upper left* indicate peak temperature of the "Tauernkristallisation" (in the east, from RSCM, Scharf 2013; in the west from von Blanckenburg et al. 1989) at 30–28 Ma (Christensen et al. 1994). The age of peak-temperature conditions in the east is assumed to be equal to the age of peak temperatures in the west (c. 30 Ma) as determined by Christensen et al. (1994). Sample localities for the Eastern Tauern Subdome are shown in Fig. 5. Closure temperatures used are as follows: Rb/Sr white mica 500 ± 50 °C (Purdy and Jäger 1976); K/Ar hornblende 530° + 33/–40 °C (Harris 1981; von Blanckenburg and Villa 1988); $^{40}Ar/^{39}Ar$ white mica 400–470 °C depending on grain size and cooling rate (Harrison et al. 2009); Rb/Sr biotite 300 ± 50 °C (Jäger et al. 1967; used in von Blanckenburg et al. 1989 and Favaro and Schuster, personal communication); ZFT 260 ± 20 °C (Foster et al. 1996; used in Fügenschuh et al. 1997; Dunkl et al. 2003 and Bertrand, personal communication) Note that we assumed a closure temperature of 500 ± 50 °C for the Rb/Sr white mica system, which is somewhat below the 550 ± 50 °C used by von Blanckenburg et al. (1989). *Vertical bar* along the time axes at 23–21 Ma indicates the probable onset of South-Alpine indentation as discussed in the text and shown in Fig. 10

Window. In general, this compilation shows that rapid cooling in the Eastern Tauern Window preceded that in the west. This generalization pertains both to the onset of rapid cooling at 550–500 °C and to the end of this period of rapid cooling when 300 °C was reached, i.e., approximately at the viscous-to-frictional transition in quartz-bearing mylonitic rocks. Cooling was rapid from 21 Ma until about 16 Ma in the KSZS and from 18 to 13 Ma in the BSZS. The zircon ages for the KZSZ and the BSZS show wide, overlapping ranges, possibly reflecting a long time spent at depths corresponding to the partial annealing zone at the end of rapid exhumation. The details of this cooling history, as well as the possible reasons for the wide range of ages, will be discussed elsewhere (Scharf 2013 and in preparation; Bertrand et al., in preparation). Next, we turn to the implications that the cooling histories have for exhumation.

At this point, we emphasize the inherent difficulty of using cooling ages to date exhumation and calculate exhumation rates in the Tauern Window. Converting

cooling rates into exhumation ages requires thermal modeling in order to account for the fact that rapidly exhuming rocks are poor heat conductors and not begin to cool significantly until they have already undergone significant exhumation (England and Thompson 1984). Such modeling is currently only available for the western part of the Tauern Window (Fügenschuh et al. 1997). Nevertheless, we can make the following generalizations: In the Western Tauern Subdome, thermobarometric data for a point about 5 km to the east of the Brenner Normal Fault and at the base of the BSZS indicate that exhumation was slow (<1 mm/a) until about 20 Ma (von Blanckenburg et al. 1989; Fügenschuh et al. 1997). Thereafter, the exhumation rate of this point increased rapidly to 4 mm/a and remained high (2–4 mm/a) until about 15 Ma, when it decreased to 1 mm/a.

At present, there are no good constraints on the onset of rapid exhumation in the eastern part of the Tauern Window; if we assume a similar time lag between the onset of rapid exhumation and cooling as in the west, then rapid exhumation in the east probably began no earlier than 23 Ma. Certainly, rapid exhumation in the east began no later than the onset of rapid cooling there at 21 Ma.

The modeled onset of rapid exhumation along the BSZS at 20 Ma (Fügenschuh et al. 1997) fits well with biostratigraphic evidence from within the Giudicarie Belt (Fig. 1) that accommodated impingement of the Eastern Alps by the Adriatic indenter (Ratschbacher et al. 1991b; Rosenberg et al. 2004; Pomella et al. 2011, 2012). Locally, i.e., in the Monte Brione area, deformation postdated pelagic sedimentation until 21.5 Ma (Luciani and Silvestrini 1996; Schmid et al., in press). When considering the entire deformed area within the Giudicarie Belt, including the kinematically related Milano Belt, indentation may have begun already at 23 Ma (age of the youngest sediments in the Monte Orfano area, Sciunnach et al. 2010). The resulting 23–21 Ma age range for the onset of indentation is indicated with a black bar on the time axis of Fig. 7. The lag of 2 Ma between the onset of rapid exhumation (20 Ma) and rapid cooling (18 Ma) in the west is consistent with the idea that the rise of rapidly exhuming rocks is nearly adiabatic before rapid cooling sets in (e.g., England and Thompson 1984). In contrast, the sheared margin of the Eastern Tauern Subdome began to cool rapidly some 3 Ma earlier than in the west and at about the same time that indentation began along the Giudicarie Belt in the Southern Alps. If one assumes that most exhumation and cooling along the KSZS is related to such indentation and very little of it to earlier periods of exhumation following the 30–28 Ma "Tauernkristallisation" (Selverstone 1988), then exhumation rates in the Eastern Tauern Subdome must have been very high already before 21 Ma, i.e., before the time interval of rapid cooling in the KSZS lasting from 21 to 16 Ma. On the other hand, the sheared margin of the Western Tauern Subdome was still exhuming slowly before 20 Ma, as discussed below and depicted in Fig. 7 (von Blanckenburg et al. 1989; thermal modeling of Fügenschuh et al. 1997). In summary, exhumation and cooling rates appear to be similar but diachronous in Eastern and Western Tauern Subdome.

A possible explanation of the different timing of exhumation and/or cooling for the KSZS and BSZS at either end of the Tauern Window may be that exhumation initiated at different stages of the indentation process and/or that differences in the cooling history reflect different relative contributions of folding, normal faulting and erosion toward the exhumation. In the latter case, exhumation in the west involved predominantly high-amplitude folding and rapid erosion, whereas in the east, the lower fold amplitudes suggest that normal faulting along the KSZS accommodated a greater proportion of the exhumation. The possibility that rapid exhumation in the east began almost at the same time is supported by generic thermal modeling showing that tectonic denudation involving mostly extensional faulting increases the cooling rate of the exhuming footwall and therefore decreases the time lag between rapid exhumation and rapid cooling (Ruppel et al. 1988).

In summary, the Penninic–Subpenninic nappe stack in the entire Tauern Window probably underwent slow exhumation (<1 mm/a) and cooling at high temperatures (630–500 °C) between 30 Ma (Selverstone 1988) and the onset of rapid exhumation somewhere within the 23–21 Ma time range. Cooling in response to fast exhumation begun earlier in the east, possibly because extensional faulting predominated as a mechanism of exhumation along the KSZS while exhumation along the BSZS involved primarily doming and erosion. Alternatively, the younger ages of rapid cooling in the west (18–13 Ma) than in the eastern part of the Tauern Window (21–16 Ma) may reflect basic differences in mode of indentation and resulting exhumation, as discussed below ("Strain partitioning between folding, normal faulting and strike-slip faulting in the Eastern Tauern Window" section).

Strain partitioning between folding, normal faulting, and strike-slip faulting in the Eastern Tauern Window

Coeval folding, normal faulting, and stretching

At first glance, the arcuate trend and variable dip of the KSZS around the perimeter of the Eastern Tauern Subdome seem to indicate that extensional shearing preceded folding. However, later folding of the KSZS can be ruled out because the KNF is not folded (undeformed contours in

Fig. 2a). Moreover, the coincidence of maximum tectonic omission of footwall units along the KNF with the broad hinge of the Eastern Tauern Subdome indicates that folding and extensional shearing must have been coeval (Fig. 3). This interpretation is also consistent with the asymmetrical, concentric pattern of peak-temperature isotherms (Fig. 5) and Miocene mineral cooling ages in the Eastern Tauern Subdome (Luth and Willingshofer 2008). In the following, we show how the normal faulting along the KNF and strike-slip faulting along the two orogen-parallel branches of the KSZS are kinematically linked to the formation of the Eastern Tauern Subdome.

The northern and southern branches of the KSZS as stretching faults

We interpret the steeply dipping northern and southern branches of the KSZS as stretching faults in the sense of Means (1989, 1990). Stretching faults are characterized by different displacement gradients on either side of the fault, such that the offset of markers can increase from zero at one end to a maximum value at the other. Kurz and Neubauer (1996) already proposed that a branch of their dextral "Mölltal Valley Fault" (not identical with our Mölltal Fault) is a stretching fault whose offset increases southeastward along the Sonnblick Lamellae (Fig. 2) to a total of 24 km as estimated from the dextral offset of Austroalpine basal thrust (see their Fig. 12). Expanding on this concept, we propose that the steep northern and southern branches of the KSZS are stretching faults that accommodated some 26 km of orogen-parallel extension along the KNF ("Displacement along the KSZS" section).

As shown in "Katschberg Shear Zone System" section, these two branches are marked by orogen-parallel strain gradients as manifested by an increase in width and decrease in spacing of mylonitic structures (foliation, stretching lineation) going from the ends of these branches in the west to where they bend into the KNF in the east (Fig. 2). We note that sinistral shear along the southern branch including the Sonnblick Lamellae is unrelated to dextral shear along the Mölltal Fault. This is contrary to the interpretation of Kurz and Neubauer (1996) who regarded the Sonnblick Lamellae as an integral part of their dextral "Mölltal Valley Fault". Further to the northwest in the vicinity of the Sonnblick Dome, the coexistence of sinistral and dextral kinematic indicators reveals that the component of coaxial strain is more pronounced there. The analogous observations made along the dextral northern branch of the KSZS ("Katschberg Shear Zone System" section) suggest that this branch is also a stretching fault. Together, these branches accommodated orogen-parallel extension of the core of the Eastern Tauern Subdome with respect to the un- or less-deformed Austroalpine units north and south. These units also accommodated eastward lateral extrusion further to the east, as discussed below.

Faults in the Austroalpine basement and their bearing on indentation of the Eastern Tauern Subdome

At first sight, dextral offset across the brittle Mölltal Fault appears to have post-dated sinistral mylonitic shearing along the southern branch of the KSZS. However, a closer inspection of the large-scale kinematics of the Tauern Window (Fig. 8), particularly of the Eastern Tauern Window, indicates that this faulting and shearing must have been contemporaneous, as discussed below and shown in Fig. 9.

During northward motion of the Southern Alps indenter east of the Giudicarie Belt, the Austroalpine units located between the Tauern Window and the Periadriatic Fault were fragmented into relatively rigid, wedge-shaped blocks. These are separated by strike-slip faults that accommodated moderate orogen-parallel extension (Fig. 8; Frisch et al. 1998; Linzer et al. 2002). According to Schmid et al. (in press), the Miocene Zwischenbergen-Wöllatratten (Exner 1962c) and Drautal Faults (Heinisch and Schmidt 1984) were originally a single sinistral strike-slip fault (ZWD in Fig. 8) that offsets the Defferegen-Antholz-Vals (DAV) Fault. The DAV and Ragga-Teuchel (RT) Faults are interpreted as segments of the same pre-Miocene fault because they juxtapose identical Austroalpine units (labeled 1 and 2 in Fig. 8) and define the southern boundary of Late Cretaceous Eo-alpine metamorphism (SAM of Hoinkes et al. 1999). The RT Fault was active in pre-Miocene time as indicated by undeformed dykes with intrusive ages of 40–30 Ma (Deutsch 1984) that cut its fault plane (Hoke 1990). Thus, the available data indicate that the Rieserferner- and Drau-Möll blocks individuated in Miocene time, i.e., during doming and extensional exhumation of the Eastern and Western Tauern subdomes.

The sinistral ZWD Fault is conjugate with respect to the dextral Mölltal Fault and both merge with the Periadriatic Fault along the northern margin of the Southern Alps indenter. These conjugate faults must be considered as cogenetic because our structural data show that they meet in a broad zone of cataclasites at their point of intersection near Obervellach. We found no trace of the Mölltal Fault west of Obervellach within or along the northern margin of the Sonnblick Dome (as discussed in "Brittle faulting" section), so we propose that the western end of the Mölltal Fault at its junction with the ZWD Fault marks a point of zero fault displacement (Fig. 9). This point at the apex of the wedge-shaped Drau-Möll Block is close to the northwestern end of the sinistral southern branch of the KSZS, where we have shown that displacement related to Katschberg shearing and extension is also at or near zero. This

coincidence is compounded by almost identical amounts of northwest to southeast-directed displacement for the KSZS and the Mölltal Fault (Fig. 9): The Mölltal Fault accommodated some 24 km dextral offset of the Austroalpine basal thrust (vector *v* in Fig. 9; Kurz and Neubauer 1996), while the southern KSZS accommodated about 26 km of extension across the KNF (vector w in Fig. 9) according to our estimates above ("Displacement along the KSZS" section). These are strong kinematic arguments that northward indentation of the Drau-Möll Block caused orogen-parallel stretching of the exhuming Eastern Tauern Subdome and that the Mölltal Fault and southern KSZS behaved collectively as a stretching fault. In this scenario, units in the footwall of the KSZS extruded eastward with respect to the apex of the indenting Drau-Möll Block. Lateral extrusion provided room for extension and exhumation of the Eastern Tauern Subdome during north–south shortening. If the present-day width of the eastern margin of the Eastern Tauern Subdome is assumed to approximate its original width (line *x* in Fig. 9) and the length of the KNF when it is nucleated is a line connecting points of zero displacement at the ends of the northern and southern KSZS (line *y* in Fig. 9), then the subdome is estimated to have undergone about 12 km of shortening during orogen-parallel stretching. This is certainly a minimum estimate because line x includes the Hochalm- and Rotgülden folds. However, 12 km corresponds to the shortening vector in the same direction obtained from the offset along the ZWD Fault (vector *z* in Fig. 9), suggesting that the contribution of folding and erosion was modest compared to that of extension across the KNF. Note, however, that the total amount of orogen-perpendicular shortening caused by indentation of the Adriatic microplate is significantly greater and increases to the west, reaching 80 km along a line parallel to the Giudicarie Belt (Linzer et al. 2002).

Comparison with the Western Tauern Window and strain partitioning at the scale of the entire Tauern Window

Orogen-parallel stretching and folding have also been shown to be coeval in the Western Tauern Subdome (e.g., Fügenschuh et al. 1997; Rosenberg and Schneider 2008) which is framed by the Brenner Shear Zone System (BSZS). In detail, the BSZS consists of the Brenner Normal Fault, the sinistral Tauern Northern Boundary (TNB) Fault (Töchterle et al. 2011), and the dextral Sterzing-Mauls (SM) Fault (Schmid et al., in press). North of the Tauern Window, the sinistral Salzach-Ennstal-Mariazell-Puchberg (SEMP) strike-slip fault ends westward in a zone of diffuse sinistral shearing within the Tauern Window (i.e., the Ahorn Fault of Rosenberg and Schneider 2008; see Fig. 8). Thus, the SEMP Fault plays a major role during the exhumation of the Western Tauern Subdome (Rosenberg and Schneider 2008). Assessing the relative importance of strike-slip faulting and normal faulting in accommodating orogen-parallel stretch is difficult in the case of the Western Tauern Subdome, primarily due to difficulty in estimating the extensional offset on the Brenner Normal Fault; recent estimates of this extension vary from 2 to 14 km (Rosenberg and Garcia 2011) to 44 km (Fügenschuh et al. 2012), but are much less than the previous minimum estimate of as much as 70 km (Fügenschuh et al. 1997).

The most straightforward approach to assessing the amount of east–west extension on the Brenner Normal Fault invokes the 66 km of sinistral displacement along the SEMP Fault and its splay, the Königsee-Lammertal-Traunsee (KLT) Fault (Fig. 8; Linzer et al. 2002; Rosenberg and Schneider 2008; Schmid et al., in press). This total displacement of 66 km must reduce to zero toward the BSZS, i.e., westward along strike of the Ahorn Fault and other sinistral strike-slip zones (Schneider et al., in press) that terminate as steep, diffuse mylonitic shear zones in the footwall of the Brenner Normal Fault. Hence, the SEMP Fault and its diffuse branches in the Western Tauern Subdome can be interpreted as a stretching fault in the sense of Means (1989). This implies a WSW–ENE directed stretch of the Western Tauern Window of some 66 km. By adding the extension accommodated by the brittle part of the Brenner Normal Fault (between 2 and 14 km according to Rosenberg and Garcia 2011; some 4–5 km according to Fügenschuh et al. 1997, their Silltal Fault) which is kinematically independent of the SEMP Fault, we estimate that the total amount of orogen-parallel stretch in the Western Tauern Subdome is about 70 km. This stretching was contemporaneous with an estimated 32 km of orogen-perpendicular north–south shortening in this part of the Tauern Window (Schmid et al., in press).

Most of this orogen-parallel stretch within the Western Tauern Window must be seen in the context of sinistral transpression in front of the Southern Alps indenter, more specifically, at the western edge of the Rieserferner Block (Fig. 8) as observed in analog indentation experiments (Ratschbacher et al. 1991b; Rosenberg et al. 2007). Folds and shear zones in the Western Tauern Subdome form a predominantly sinistral, transpressional shear system that is continuous at both ends with the Giudicarie- and SEMP Faults (Fig. 1). The similarity of 80 km of NNE-directed displacement on the Giudicarie Belt, including the Meran-Mauls (MMF) Fault (Frisch et al. 2000; Linzer et al. 2002), and the aforementioned estimate of 70 km of east–west extension accommodated by the BSZS and related strike-slip faults are consistent with the idea that the Western Tauern Subdome served as a bridge structure in transferring much of the motion of the South-Alpine indenter to eastward lateral extrusion in the Tauern Window (Rosenberg and Schneider 2008).

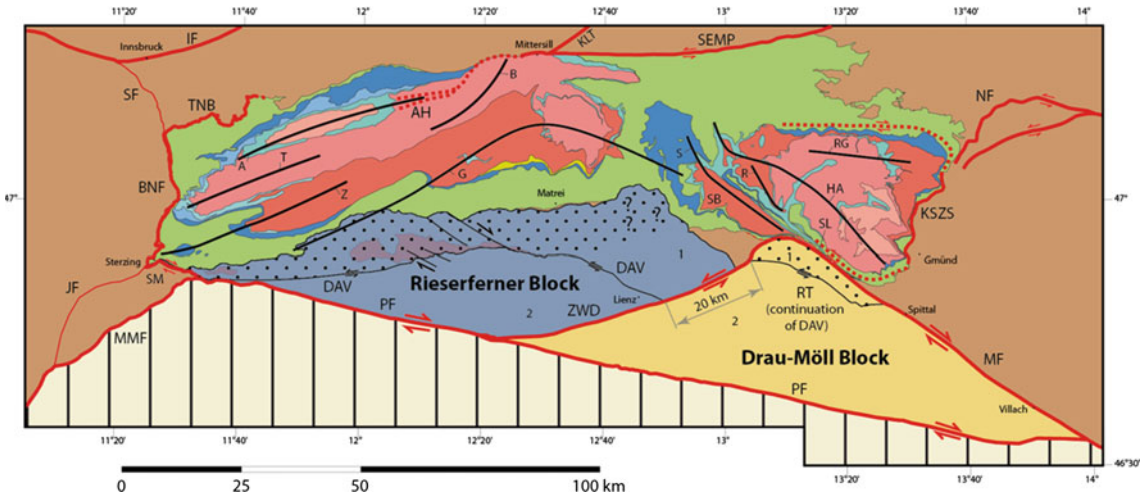

Fig. 8 Tectonic map simplified from Fig. 1 showing the major folds and faults within and around the Tauern Window, in particular, the fragmented triangular zone of upper Austroalpine units south of the Tauern Window made up of the Drau-Möll Block (*yellow unstippled*) and the Rieserferner Block (*blue unstippled*). *Thick red lines* indicate strike-slip zones that were instrumental for indentation and exhumation of the Tauern Window. Stippled pattern: Austroalpine crust at the leading edges of the blocks that were affected by Eocene/Oligocene temperatures >375 °C on the western, Rieserferner side (Rb/Sr, K/Ar biotite cooling ages, compiled in Luth and Willingshofer 2008) and >300–270 °C on the eastern, Drau-Möll side (Zircon Fission Track, Wölfler et al. 2008). Tectonic units: *1* Koralpe-Wölz Nappe System, *2* Drauzug-Gurktal Nappe System. Folds and Domes: *A* Ahorn, *B* Breitfuss, *G* Granatspitz, *HA* Hochalm, *R* Romate, *RG* Rotgülden, *SB* Sonnblick, *SL* Sonnblick Gneiss Lamella, *T* Tux, *Z* Zillertal. Faults and shear zones: *AH* Ahorn Shear Zone, *ASZ* Ahrntal Shear Zone, *BNF* Brenner Normal Fault, *DAV* Defferegen-Antholz-Vals Fault, *GSZ* Greiner Shear Zone, *IF* Inntal Fault, *JF* Jaufen Fault, *KLT* Königsee-Lammertal-Traunsee Fault, *KSZS* Katschberg Shear Zone System, *MF* Mölltal Fault, *MMF* Meran-Mauls Fault, *NF* Niedere Tauern Southern Fault, *PF* Periadriatic Fault, *RT* Ragga-Teuchel Fault, *SEMP* Salzach-Ennstal-Mariazell-Puchberg Fault, *SF* Silltal Fault, *SM* Sterzing-Mauls Fault, *TNB* Tauern Northern Boundary Fault, *ZWD* Zwischenbergen-Wöllatratten and Drautal Faults

In summary, orogen-parallel stretch (70 km) in the Western Tauern Window is greater than in the Eastern Tauern Window (26 km, Fig. 9). Also, the kinematic link of stretching in the west to strike-slip faulting on the SEMP Fault is consistent with overall dextral transpression in the west, in contrast to the predominance of sinistral transpression in the east, where motions are unrelated to displacement on the SEMP Fault. This is in accord with the strain patterns seen in analog indentation models (Ratschbacher et al. 1991b; Rosenberg et al. 2007).

Strain partitioning in the Tauern Window is intimately related to the geometry of the two, wedge-shaped blocks of Austroalpine basement between the Tauern Window and the Periadriatic Fault (Fig. 8): the Rieserferner- and Drau-Möll blocks. These blocks are characterized by brittle Eocene/Oligocene deformation at low temperatures and are delimited from their warmer and ductilely deformed leading edges (stippled domains in Fig. 8) by major Late Oligocene shear zones (Fig. 8, DAV Fault, e.g., Borsi et al. 1978; Wagner et al. 2006; RT Fault, Hoke 1990). These leading edges underwent penetrative greenschist-facies mylonitization and upright folding at temperatures above the frictional-viscous transition in quartz (Wagner et al. 2006). This deformation is continuous with the upright folding in the Tauern Window (Wagner et al. 2006). Thus, based on these strong contrasts in strain intensity that existed in Early Miocene times, we infer that the colder Austroalpine blocks were more rigid than the warm, ductilely deforming orogenic crust to the north. This explains why the former accommodated so much less orogen-parallel stretch (50 km = stretch associated with offsets of c. 10 km on the SM Fault, 16 km on the ZWD Fault and 24 km on the Mölltal Fault in Figs. 8, 9) than the Penninic units in the Tauern Window (about 100 km, i.e., 70 and 26 in the Western and Eastern Tauern subdomes, respectively, see above).

The indentation of these Austroalpine blocks also had a pronounced effect on the pattern of shortening and exhumation of orogenic crust in the Tauern Window. The apex of the Rieserferner Block coincides with the area where Miocene north–south shortening is a minimum and where no Subpenninic units were exhumed. Shortening and orogen-parallel extension in front of the northeastern side of the Drau-Möll Block further east is by far greater as indicated by the impressive thinning of the elongate Sonnblick Dome to the narrow Sonnblick Gneiss Lamellae (20 km long, 0.5 km wide, Exner 1962b; Fig. 2b). North–south shortening is also intense at the southern margin of the Western Tauern Subdome, adjacent to the northwestern side of the Rieserferner Block, where folds are tight to isoclinal with km-scale amplitudes (Brandner et al. 2008; Rosenberg and Garcia 2011; Schmid et al., in press; their Fig. 3).

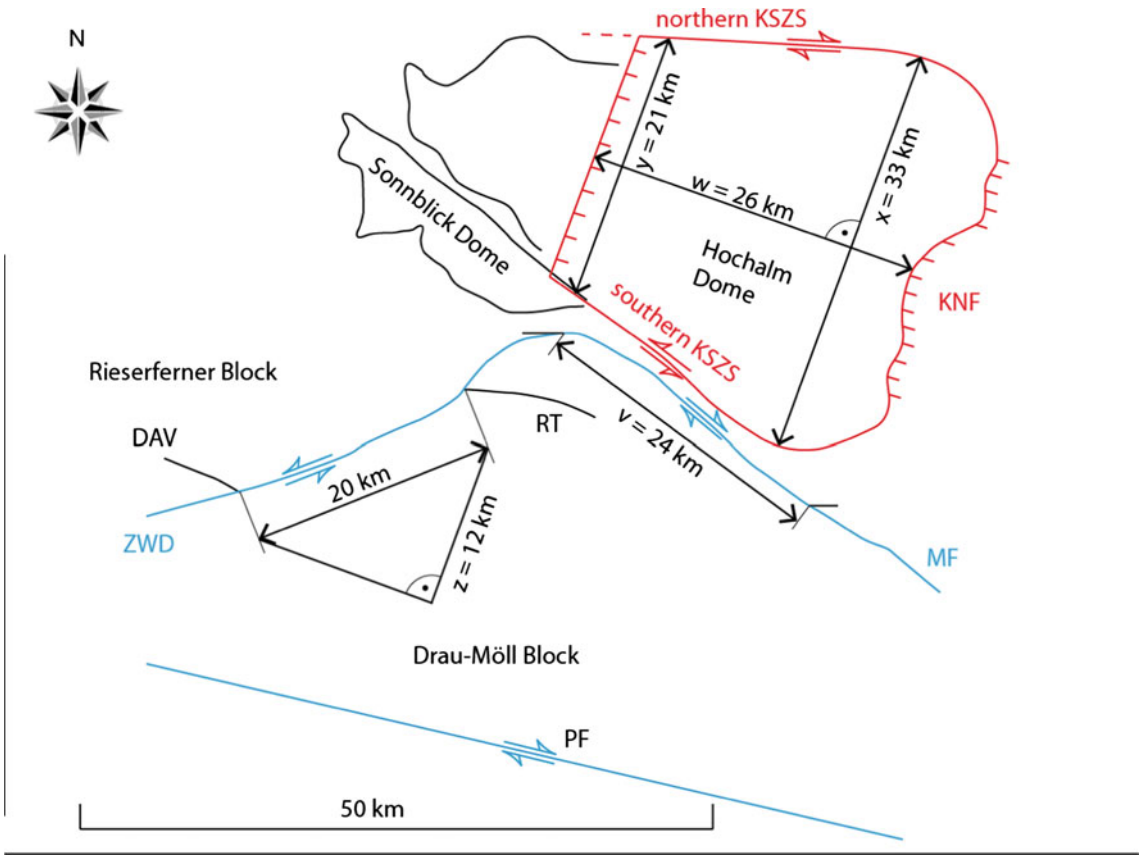

Fig. 9 Semi-quantitative evaluation of strain partitioning during coeval shortening and orogen-parallel stretch of the Eastern Tauern Window. See Fig. 8 for location of the figure and text for the discussion of the vectors shown: *v* offset of the eastern margin of the Sonnblick Dome with respect to the western margin of the Hochalm Dome, achieved along the stretching segment of the Mölltal Fault that nucleated at the southern margin of the Sonnblick Dome, *w* orogen-parallel stretch within the Tauern Window achieved by the KSZS, *x* width of the KSZS and Eastern Tauern Subdome at its present-day eastern margin, *y* width of the KSZS at the suspected site of its nucleation at about 21 Ma, *z* additional component of orogen-perpendicular shortening achieved by sinistral offset between Rieserferner- and Drau-Möll blocks during indentation. See Fig. 8 for abbreviations of faults and shear zones. Colored faults: *red* branches of the KSZS, including the KNF, *blue* faults bounding the Drau-Möll Block

Relationship of lateral extrusion to Adria-Europe convergence

Timing constraints

Figure 10 summarizes the age of the main tectonic events in the Tauern Window, the sedimentary basins in the Eastern Alps and the Pannonian Basin. To place these events in a larger kinematic context, we include the age of sinistral offset along the Guidicarie Belt at the western edge of the South-Alpine indenter, deformation within the Southern Alps and on counterclockwise rotation of the Adriatic microplate with respect to Europe. The onset of Alpine collision and breakoff of the European slab in Late Eocene to Early Oligocene times (e.g., von Blanckenburg and Davies 1995; Schmid et al. 1996) coincides with nappe stacking and duplex formation of the Penninic units in the Tauern Window, including units that were exhumed from high-pressure metamorphic conditions (Ratschbacher et al. 2004; Kurz et al. 2008). The Adriatic microplate moved to the northwest with respect to both Europe and Africa throughout Cenozoic time, but at about 20 Ma, i.e., at around the time when indentation of the Southern Alps began, the rate of convergence with Europe dropped from 1.3 mm/a to <0.5 mm/a (Handy et al. 2010).

As discussed earlier, constraints on the age of indentation (post 21.5 Ma) are provided by an Oligo-Miocene pelagic sequence from within the Giudicarie Belt that lies to the east of the Guidicarie Fault and accommodated southeast-directed thrusting and indentation (Fig. 1). A somewhat earlier start of indentation at around 23 Ma (Fig. 10) is indicated by south-directed thrusting in the western part of the Southern Alps (Milano Belt) that is kinematically linked with the sinistral Giudicarie Belt and that post-dates the intrusion of the Adamello Pluton (Schönborn 1992; Schumacher et al. 1997; Sciunnach et al. 2010). The Milano Belt is sealed by the Messinian unconformity beneath the Po Plain (5 Ma; Pieri and Groppi

1981). Older thrusting in the western Southern Alps preceded the Adamello intrusion and was active in Late Cretaceous and Early to Middle Eocene times (Zanchi et al. 2012). The eastern Southern Alps, i.e., east of the Giudicarie Belt, were first affected by southwest-vergent Paleocene and Eocene thrusts of the most external Dinarides then later by S to SSE-directed "Alpine" thrusts that have been active since Serravallian (according to Castellarin and Cantelli 2000), or alternatively, since Tortonian time (according to Venzo 1940; Doglioni and Bosellini 1987; Schönborn 1999; Nussbaum 2000). Either way, this was certainly after rapid exhumation of units in the Tauern Window and possibly even after the offset of the Periadriatic Fault along the Giudicarie Belt (Fig. 10). These substantial differences between western and eastern Southern Alps, particularly since Miocene time, suggest that the latter remained rigid during indentation between 21 and 13–10 Ma (see Fig. 10).

In Austroalpine units east of the Tauern Window, strike-slip faulting related to the opening of transtensional and pull-apart basins began in the Late Early Miocene and overlapped in time with rapid exhumation and cooling of the Eastern and Western Tauern subdomes (Fig. 10). The intramontane basins along the sinistral Niedere Tauern Southern (NF) Fault (Tamsweg-, Seetal-, Fohnsdorf Basins; Fig. 1) that formed in the hanging wall of the KSZS ("Brittle faulting" section) opened between 17.3 and 16.7 Ma, with sedimentation lasting to 14.3–12.8 Ma (Zeilinger 1997; Sachsenhofer et al. 2000; Strauss et al. 2001). Their opening post-dated the onset of extensional subsidence in the Styrian Basin (18.2 Ma) where syn-rift subsidence ended at 12 Ma (Sachsenhofer et al. 1997). Pull-apart in the Vienna Basin started even later, at 16 Ma, after an earlier period of wedge-top sedimentation and ended at 7.6 Ma (Figs. 1, 10; Decker 1996; Bechtel et al. 2007; Hölzel et al. 2010; Paulissen et al. 2011). Rifting in the Styrian- and Vienna basins was related to rifting in the Pannonian Basin (e.g., Horváth et al. 2006). The Lavanttal Basin along the dextral transtensional fault of the same name (Fig. 1) was initially (16.7–12 Ma) part of the Styrian Basin but became separated from the latter by the Lavanttal Fault at 12–5 Ma (Reischenbacher et al. 2007; Kurz et al. 2011; Wölfler et al. 2010).

It is important to note that the subsidence related to rifting in the Pannonian Basin located within the Intra-Carpathian Arc (inset to Fig. 1) started earlier (Eggenburgian, 20 Ma) than in the Austroalpine domain and lasted until Badenian time (about 15 Ma) based on intrabasinal unconformities (Horváth et al. 2006, U1–U2 in Fig. 10). In contrast, syn-rift sedimentation lasted longer in the Lavanttal-, Styrian-, and Vienna basins (Fig. 10). The Pannonian Basin underwent post-extensional thermal subsidence until Late Serravallian time (12 Ma) and has experienced inversion, renewed thermal subsidence, and renewed basin inversion since the Late Pliocene (Horváth et al. 2006).

Taken together, the age relations in Fig. 10 suggest that rapid exhumation and orogen-parallel extension in the Tauern Window coincided with north-directed motion of the South-Alpine indenter along the Giudicarie Belt beginning sometime between 23 and 21 Ma. Most importantly, the strike-slip tectonics associated with the opening of intramontane basins in the Eastern Alps is somewhat younger than back-arc extension and subsidence of the Pannonian Basin. This makes roll-back subduction beneath the Carpathians an unlikely trigger of Neogene exhumation in the Tauern Window. We will return to this important point in our final analysis ("Implications for the forces driving lateral extrusion" section), but turn next to the kinematics of indentation and lateral extrusion.

Kinematics and amount of lateral extrusion during indentation

We envisage four stages of convergence and lateral extrusion, shown schematically in Fig. 11a–d:

1. Crustal thickening and formation of an Alpine orogenic root started with the onset of subduction of the European continental lithosphere at about 40 Ma in the Tauern Window (e.g., Schmid et al. 1996; Kurz et al. 2008; Wiederkehr et al. 2009; Handy et al. 2010). This led to the formation of km-scale duplex structures that involve Subpenninic basement nappes derived from the European continental margin at around 32–30 Ma (Schmid et al., in press). Thickening also affected the Austroalpine units north of the DAV Fault, as evidenced by Paleogene mineral cooling ages (e.g., Luth and Willingshofer 2008; Wölfler et al. 2011) and by Oligocene granitoids whose intrusive depths place a lower limit on the maximum thickness of the crust at that time (25 km in the case of the Rensen Pluton, Rosenberg et al. 2004 and references therein). We interpret this intrusive activity to have been triggered by Late Paleogene rupturing of the south-dipping European slab beneath the Central and Eastern Alps (von Blanckenburg and Davies 1995).
   Coeval strike-slip motion on the dextral Periadriatic Fault (Schmid et al. 1989), the sinistral DAV Fault (Kleinschrodt 1987; Müller et al. 2001), the sinistral Paleo-Inntal Fault (Ortner and Stingl 2003), and the Engadine Fault (Schmid and Froitzheim 1993) may have coincided with the onset of slow exhumation of the Venediger Nappe System as early as 29 Ma (Selverstone et al. 1995). This suggests that the Alpine orogenic crust beneath the future Tauern Window already began to spread laterally during Oligocene time (Fig. 11a).

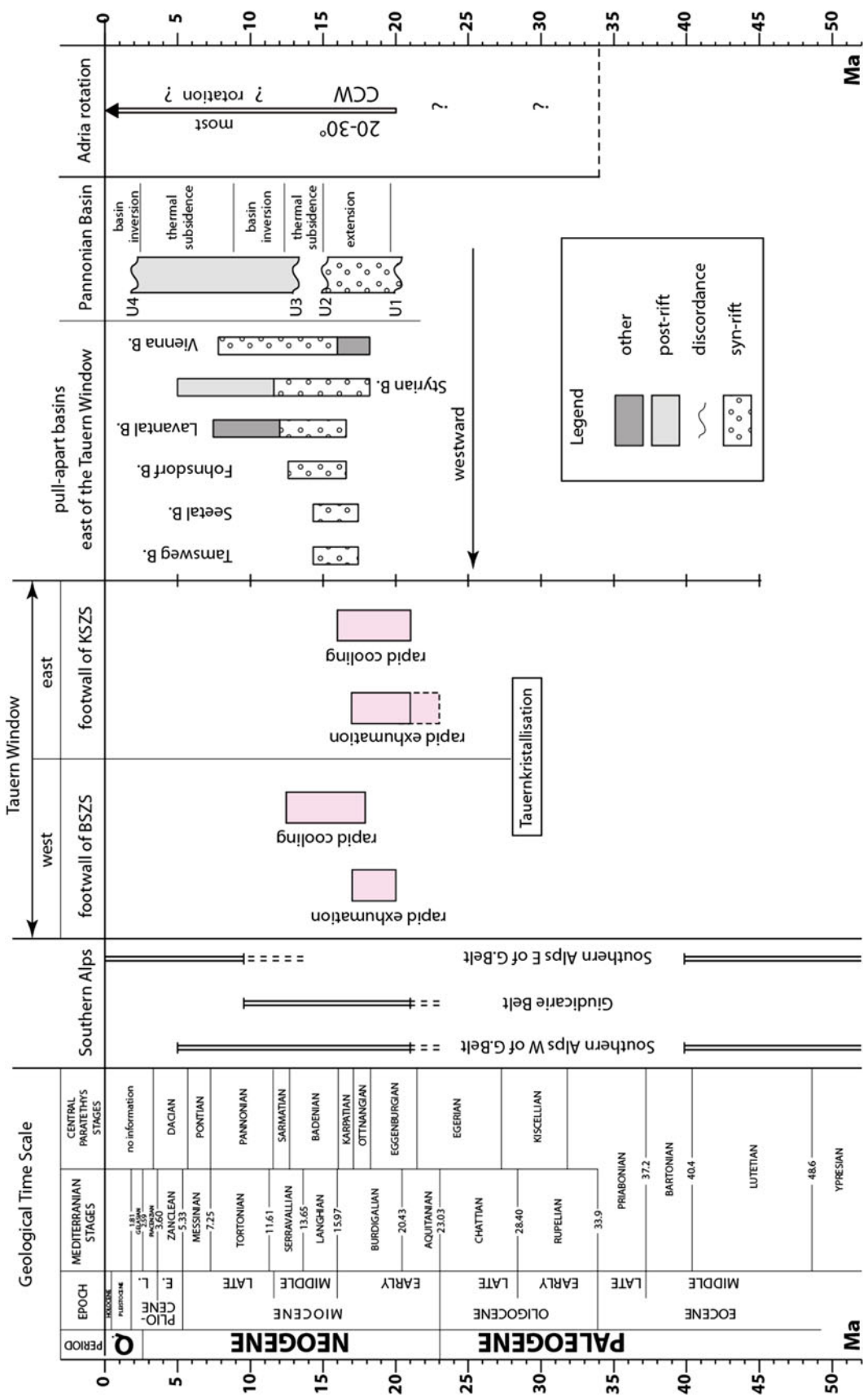

Fig. 10 Timing of events related to exhumation and lateral extrusion in the Eastern Alps: sinistral motion and indentation along the Giudicarie Belt, post-nappe folding and extensional shearing in the Tauern Window, basin formation and strike-slip faulting east of the Tauern Window, subsidence and opening of the Pannonian Basin, rotation of the Adriatic microplate (see text for further discussion and references). Geological time scale: Mediterranean stages from Gradstein et al. (2004); central Paratethys stages from Piller et al. (2007) and Steininger and Wessely (2000)

2. Early Miocene indentation of the Adriatic microplate triggered coeval doming and extensional shearing of the still-thickening Venediger nappe stack in the Tauern Window (Fig. 11b). Rapid exhumation (2–4 mm/a) of the nappe stack in the Western Tauern Subdome began at about 20 Ma and lasted until about 12–10 Ma in the footwall of the BSZS (Fügenschuh et al. 1997). Broadly coeval exhumation of the Eastern Tauern Subdome in the footwall of the KSZS is possible and seems reasonable in light of analog models (Ratschbacher et al. 1991a; Rosenberg et al. 2007) showing that the observed pattern of north–south shortening and east–west, orogen-parallel extension in the Tauern Window (Handy et al. 2005) was established simultaneously during coherent motion of a semi-rigid South-Alpine indenter. The exact direction of indentation, as well as the possible rotation of the South-Alpine indenter during the counterclockwise rotation of the Adriatic microplate as a whole, remains unknown. However, indentation must have been generally north-directed and oblique to the Giudicarie Fault in order to achieve transpression along the Giudicarie Belt (Fig. 1). The beginning of indentation within the 23–21 Ma time interval (Fig. 10) probably coincided with the onset of counterclockwise rotation of the Adriatic microplate and may have involved a change from south- to north-directed subduction in the Eastern Alps according to some authors (Horváth et al. 2006; Ustaszewski et al. 2008; however, see Mitterbauer et al. 2011 for an alternative interpretation invoking uniform-sense subduction). As discussed earlier and shown in Fig. 11d, the total offset along the Giudicarie Fault is about 80 km (Fig. 11a; e.g., Pomella et al. 2011 and references therein). We note that Miocene fragmentation of the Austroalpine basement south of the Tauern Window into two wedge-shaped blocks (Figs. 8, 11b–d) allowed for differential north–south shortening in front of the South-Alpine indenter while accommodating about 100 km of east–west extension of orogenic crust in the Tauern Window as discussed above. Orogen-parallel extension of the Austroalpine units is less (some 50 km, as discussed above) and increases eastward from the northwestern corner of the South-Alpine indenter (Fig. 11b), indicating that this part of the Periadriatic Fault was a stretching fault during Miocene time. Given that this segment of the Periadriatic Fault remained straight during indentation, the wedge-shaped Austroalpine blocks must have deformed somewhat in order to maintain compatibility with the South-Alpine indenter to the south.
3. By 15 Ma (Fig. 11c), the rate of exhumation had slowed considerably (Fügenschuh et al. 1997). Recent radiometric dating of sinistral shear zones in the Western Tauern Subdome indicates that shearing and isoclinal folding at the northern and southern margins of this subdome (Ahorn- and Ahrntal faults, Fig. 11b, c) stopped at 19–16 Ma as deformation localized in the core of the subdome before ending at about 10 Ma (Schneider et al., in press). The 100 km of orogen-parallel stretch across the BSZS and KSZS must be regarded as a minimum estimate because it does not include an unknown amount of stretching parallel to the post-nappe fold axes in the Tauern Window or, for that matter, any extension east of the Tauern Window in the hanging wall of the KSZS (e.g., along the Niedere Tauern Southern-, Mölltal-, and the Lavanttal faults). Hence, the total amount of Miocene east–west extension north of the South-Alpine indenter may well more than 100 km, which is generally compatible with previous estimate of Linzer et al. (2002) of about 120 km. We note that the 170 km postulated by Frisch et al. (1998) also includes extension west of the BSZS prior to indentation (Fig. 11a).

   The opening of intramontane pull-apart basins along strike-slip faults in the Austroalpine units east of the Tauern Window post-dated the onset of and outlasted the end of orogen-parallel extension within the Tauern Window, respectively (Fig. 10). All of these basins opened later than the Pannonian Basin (Fig. 10, not shown in Fig. 11) and partly outlasted syn-rift sedimentation in the Pannonian Basin, where intra-Carpathian back-arc extension had already yielded to thermal subsidence by 15 Ma (Royden et al. 1982; Horváth et al. 2006).
4. Inversion of the syn-rift and sag basins leading the present-day configuration (Fig. 11d) goes hand in hand with convergence due to slow counterclockwise rotation of Adria with respect to Europe (0.68°/Ma, Vrabec et al. 2006). This rotation was taken up by a system of thrusts and dextral strike-slip faults in the southernmost Eastern Alps of Carinthia and the Southern Alps of northeastern Italy and northern Slovenia (Fodor et al. 1999; Vrabec and Fodor 2006). This includes dextral transpression in the Karawanken Mountains east of the Hochstuhl (HF) Fault (Fig. 1; Polinski and Eisbacher 1992). Ages obtained so far for the timing of inversion of the Pannonian- and intramontane basins are controversial and vary between 12 Ma (onset of sedimentation in the Klagenfurt Basin in the front of the North-Karawanken Thrust that transpressively overprints the Periadriatic Fault; Polinski and Eisbacher 1992; Nemes et al. 1997) and Late Pliocene inversion in the Pannonian Basin (Fig. 10; Horváth et al. 2006). In contrast, a short-lived inversion in Sarmatian time (c. 12 Ma) is also reported for the

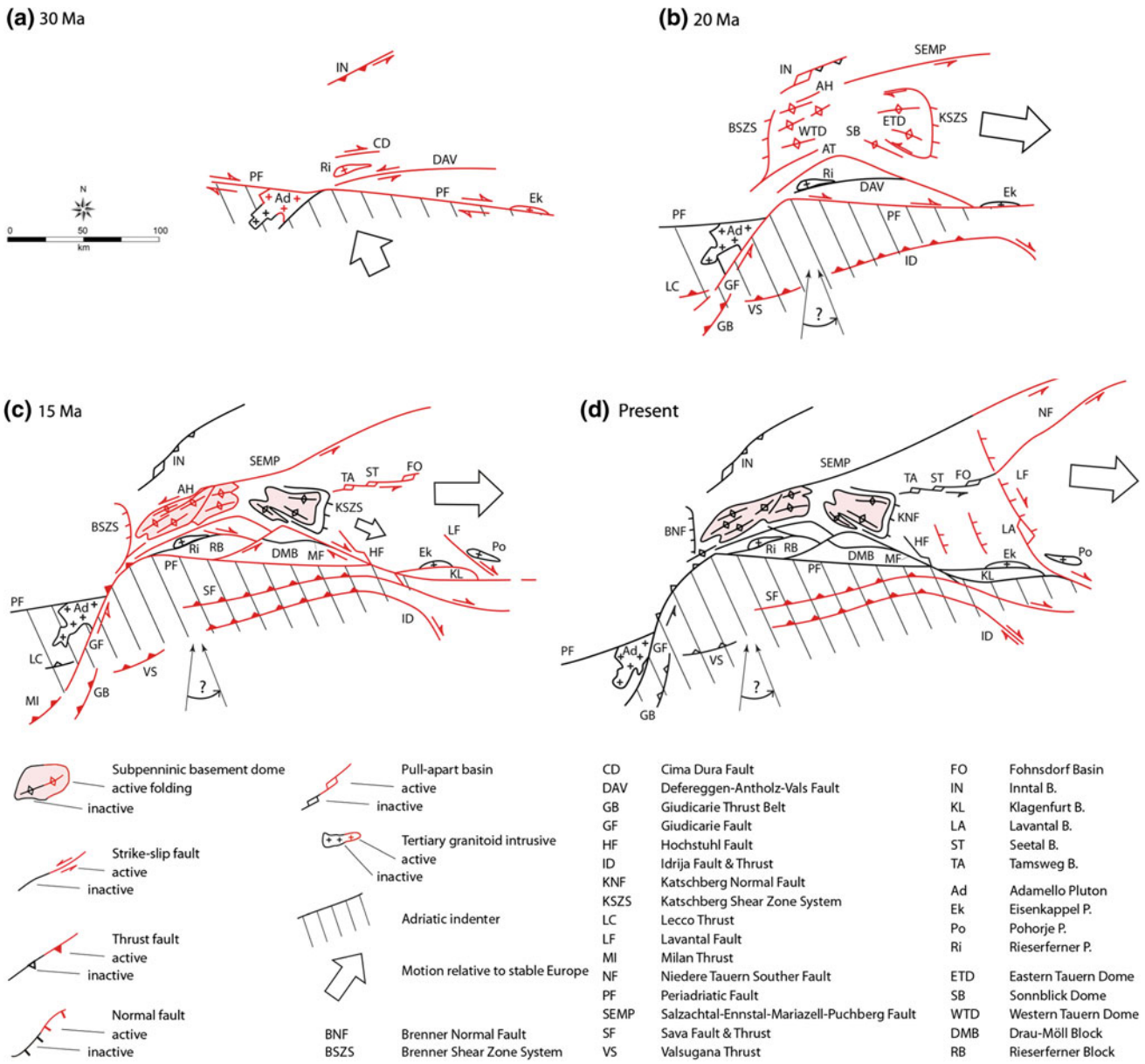

Fig. 11 Indentation and lateral extrusion in the Alps: **a** Late Alpine collision after slab-breakoff, magmatism along Periadriatic and DAV Faults, incipient doming in Tauern Window (30 Ma), **b** onset of indentation, folding, and rapid extensional exhumation of thickening orogenic crust between Katschberg- and Brenner shear zones systems, fragmentation of wedge-shaped Austroalpine units south of the Tauern Window (20 Ma), **c** continued folding, extensional exhumation and rapid cooling in the Tauern Window, strike-slip faulting of Austroalpine units east of the Tauern Window, south-directed thrusting in Southern Alps (15 Ma), **d** present situation involving oblique thrusting in Southern Alps, dextral strike-slip in northern Dinarides and lateral extrusion into the Pannonian Basin

Pannonian Basin and adjacent areas (Tomljenovic and Csontos 2001; Horváth et al. 2006). Together with radiometric age constraints for the end of indentation and lateral extrusion in the Western Tauern Subdome at 10 Ma (Schneider et al., in press), this points to the end of indentation and lateral extrusion at around 12–10 Ma. Since then, folding and faulting in the Tauern Window has stopped, with only minor seismicity recorded along the Brenner Shear Zone System (Reiter et al. 2005). East of the Tauern Window, historical and instrumentally recorded seismicity is diffuse, except for a concentration of epicenters along the Mur-Mürz strike-slip fault (Fig. 1) and in the Karawanken area (Reinecker and Lenhardt 1999). There is also evidence that the SEMP Fault is still active in sinistral strike-slip mode

(Plan et al. 2010), but the Periadriatic Fault itself is aseismic and is offset by dextral faults that merge to the east with the seismically active Hochstuhl- and Sava faults (Figs. 1, 11d). Thus, faulting that accommodates ongoing lateral extrusion has migrated yet further to the east and south of the Periadriatic Fault, whereas the Tauern Window appears to be aseismic (Reinecker and Lenhardt 1999). There is no or little evidence that the Giudicarie Belt and or the Southern Alps west of it are still active, but there is still substantial shortening ongoing in the eastern Southern Alps (e.g., Slejko et al. 1989). This can be explained partly by eastwardly increasing rates of shortening owing to the counterclockwise rotation of the Adria microplate and partly by the lateral change in present-day subduction polarity beneath the Tauern Window, i.e., near the transition from the western to the eastern parts of the Southern Alps (Lippitsch et al. 2003).

Implications for the forces driving lateral extrusion

We have argued that indentation of the Southern Alps east of the Giudicarie Belt that are part of the Adriatic microplate started at about 23–21 Ma and triggered rapid exhumation and lateral, orogen-parallel eastward extrusion that lasted until 12–10 Ma. Based on available data, this "push" of the advancing South-Alpine indenter east of the Giudicarie Belt was only assisted by east-directed "pull" of the eastwardly retreating Carpathian subduction system once westward migrating extension in the Pannonian Basin reached the vicinity of the Tauern Window at around 17 Ma. At that point, both mechanisms contributed to lateral extrusion, which involved a total of at least some 100 km orogen-parallel extension within the Tauern Window, and an additional 20 km or more east of the Tauern Window (Linzer et al. 2002) since the onset of indentation. Hence, we conclude that roll-back subduction in the Carpathians did not trigger or even assist exhumation of the Tauern Window during the initial phases of exhumation, but instead facilitated its eastward expansion via pull of the orogenic crust to the east during the later (post-17 Ma) periods of lateral extrusion. Its role was similar to that of a weak lateral constraint in the indentation experiments of Ratschbacher et al. (1991a) and Rosenberg et al. (2007).

Our data shed new light on how strain partitioned during late-orogenic indentation of orogenic crust at the eastern end of the Alps. This partitioning was governed primarily by the wedge-like shape of Austroalpine blocks at the front of the South-Alpine indenter, and by the strength contrast between these blocks and the orogenic crust presently exposed in the Tauern Window. The wedge-like shape of these semi-rigid blocks induced coeval upright folding and rapid extensional exhumation of a Late Paleogene nappe complex forming the Eastern Tauern Subdome in the footwall of the Katschberg Normal Fault. The shortening during folding was accommodated by about 26 km of eastward, orogen-parallel motion of this extensional fault along two orogen-parallel stretching faults. Exhumation therefore involved a combination of tectonic unroofing by extension faulting and erosional denudation driven by upright folding. The contribution of tectonic unroofing was greatest along the normal fault at the eastern margin of the folded nappe complex and gradually decreased away from this fault toward the central part of the Tauern Window. Compared to this situation in the east, the Western Tauern Subdome accommodated substantially more orogen-parallel extension (some 70 km) along the Brenner Shear Zone System and kinematically related strike-slip motion on the SEMP Fault.

Lateral eastward escape of the Eastern Alps east of the Tauern Window continued after 12–10 Ma, even after the Giudicarie Belt became inactive, and indeed continues today (1–2 mm/a; e.g., Bada et al. 2007) despite the fact that the Pannonian Basin is currently undergoing shortening (Grenerczy et al. 2005). This strengthens the notion that although roll-back subduction may have facilitated lateral orogenic escape in the Eastern Alps, indentation and counterclockwise rotation of the Adria plate, including the Southern Alps, was (and still is) the dominant force driving the tectonics of the Eastern Alps and adjacent areas.

Acknowledgments We are indebted to many colleagues for discussions, especially K. Hammerschmidt, S. Schneider, and C. Rosenberg, all from the Freie Universität Berlin, as well as R. Schuster and G. Pestal from the Austrian Geological Survey, Vienna. A. Giribaldi and S. Wollnik are thanked for preparing thin sections and Martina Grundmann for drafting figures. L. Ratschbacher kindly gave us Diploma theses with unpublished maps of the northeastern Tauern Window of his group. P. Brack (ETH Zürich) is thanked for making us aware of biostratigraphic data for assessing the timing of deformation within the Giudicarie Belt. The manuscript benefitted from the critical comments of the reviewers C. Teyssier and W. Kurz and of associate editor C. Rosenberg. Finally, we acknowledge the kindness and support of the National Park Services Hohe Tauern, in particular of K. Aichhorn and the staff of the Bios Zentrum in Mallnitz. Our work was financed in part by the German Science Foundation (DFG-project Ha 2403/10). S.M Schmid acknowledges the Alexander-von-Humboldt Foundation for support of his collaborative research in Berlin from 2008 to 2010.

Appendix

See Fig. 12, and Table 1.

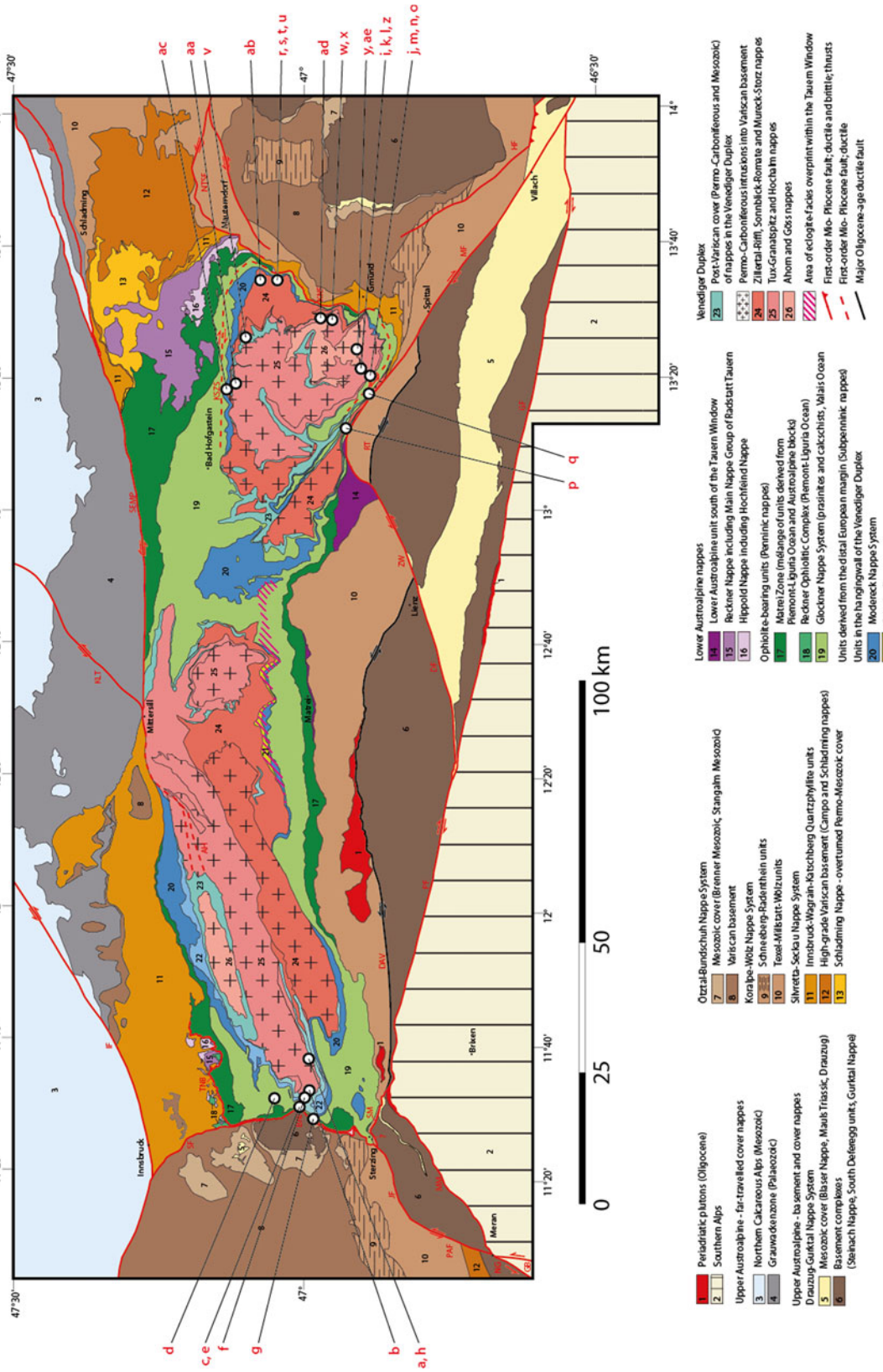

Fig. 12 Map of sample locations (*black/white circles*) used for temperature–time diagram in Fig. 8. Letters a–ae are listed in Table 1 for the corresponding ages and geochronological systems. Tectonic map taken from Schmid et al. (in press)

Table 1 Listing of all geochronological systems, ages, and their localities a–ae used for Fig. 7 (red background as shown in Fig. 12)

Data from the Brenner Shear Zone System

von Blanckenburg et al. (1989)

a Localities in Figure A-1

	PJ Pfitscher Joch		LH Landshuter Hütte		b Localities Figure A-1		
	Age (Ma)	2 sigma error (Ma)	Age (Ma)	2 sigma error (Ma)	Age (Ma)	2 sigma error (Ma)	interpretation of the age as
Rb/Sr white mica	17.6	0.2	15.6	0.4	17.6	0.2	
	20.3	0.3	19.9	0.3	20.3	0.3	
weighted mean	18.43	0.17	18.35	0.24	15.6	0.4	
					19.9	0.3	age of shearing along the Brenner Normal Fault
					weighted mean 18.41	0.14	
K/Ar white mica	PJ		LH				
	Age (Ma)	2 sigma error (Ma)	Age (Ma)	2 sigma error (Ma)	Age (Ma)	2 sigma error (Ma)	
	15.3	0.3	14.2	0.2	15.3	0.3	
	13.7	0.2	17	0.5	13.7	0.2	
weighted mean	14.19	0.17	14.59	0.19	14.2	0.2	
					17	0.5	
					weighted mean 14.37	0.12	
K/Ar biotite & Rb/Sr biotite	PJ		LH				geochronological system
	Age (Ma)	2 sigma error (Ma)	Age (Ma)	2 sigma error (Ma)	Age (Ma)	2 sigma error (Ma)	
	13	0.4	14.3	0.2	13	0.4	K/Ar biotite
	12.7	0.2	17.3	0.2	12.7	0.2	K/Ar biotite
weighted mean	12.76	0.18	17.2	0.2	14.3	0.2	K/Ar biotite
			16.27	0.12	17.3	0.2	K/Ar biotite
					17.2	0.2	K/Ar biotite
					13.2	0.8	Rb/Sr biotite
					weighted mean 15.21	0.10	

von Blanckenburg and Villa (1988)

a Localities in Figure A-1

PJ	
Age (Ma)	2 sigma error (Ma)
17.9	1
18.5	0.6
18.5	1
17	1
30.7	1.2
16.8	1
17.8	2

b Localities in Figure A-1

LH	
Age (Ma)	2 sigma error (Ma)
35.5	1.4
37.3	2
24	0.8
30.1	1.2
28.8	1.2

the authors suggest in their paper an age of 18 ± 0.8 Ma

Glodny et al. (2008)

c Localities in Figure A-1

Rb/Sr wm

	Brenner		
sample	Age (Ma)	2 sigma error (Ma)	interpretation of the age
BRE2	21	2	
TF04-30a	18.3	2.6	
PON1	17.8	1.8	
weighted mean	19.04	1.19	end of shearing along the Brenner Normal Fault

Fügenschuh et al. (1997)

ZFT		
	Age (Ma)	Localities in Figure A-1
	11	d
	10	e
	10	f
	7	g
	13	h
mean	10.2	

Table 1 continued

Data from the Katschberg Shear Zone System

Favaro and Schuster (pers. comm.)

Rb-Sr ms

	Age (Ma)	2 sigma error (Ma)	Localities in Figure A-1
	24.4	0.2	i
	21.1	0.2	j
weighted mean	22.75	0.14	

Rb-Sr bt

	Age (Ma)	2 sigma error (Ma)	Localities in Figure A-1
	17.9	0.2	k
	17.4	0.2	l
	18.1	0.2	m
	18.6	0.2	n
	17.3	0.2	o
weighted mean	17.86	0.09	

Glodny et al. (2008)

Rb/Sr white mica

Mölltal Fault

sample	Age (Ma)	2 sigma error (Ma)	Localities in Figure A-1	interpretation ot the ages as
TF04-1b	25.3	2.9	p	
TF04-5	20.7	2.3	q	age of dextral shear in mylonites
weighted mean	22.48	1.80		from the dextral Mölltal Fault

Scharf (2013)

$^{40}Ar/^{39}Ar$ laser ablation on white mica

r Localities in Figure A-1

AS1

	Age (Ma)	2 sigma error (Ma)
	15.52	1.02
	16.17	1.2
	16.34	1.52
	16.71	1.66
	17.23	0.94
	17.61	1.52
	18.04	1.26
	18.25	0.6
	18.37	0.98
	18.49	1.18
weighted mean	17.52	0.33

s Localities in Figure A-1

AS27

	Age (Ma)	2 sigma error (Ma)
	23.08	3.1
	17.53	3.18
	23.42	1.12
	23.48	1.22
	24.57	1.12
	22.86	1.38
	24.75	1.38
	19	1.48
weighted mean	23.1	0.5

t Localities in Figure A-1

AS41

	Age (Ma)	2 sigma error (Ma)
	17.76	0.98
	19.3	0.8
	18.33	0.98
	17.74	1.02
	18.92	0.56
	15.81	0.48
	18.24	0.9
	17.35	0.68
	18.5	0.64
weighted mean	18.62	1.02

u Localities in Figure A-1

AS46

	Age (Ma)	2 sigma error (Ma)
	17.87	1
	18.92	1.5
	19.08	0.64
	20	1.24
	19.74	0.94
weighted mean	19.09	0.42

v localities in Figure A-1

AS74

	Age (Ma)	2 sigma error (Ma)
	20.62	0.72
	19.47	0.82
	19.48	0.86
	20.39	0.62
	19.73	1.3
	20.77	0.82
	19.82	0.72
	18.78	1.02
	19.13	0.84
	20.19	0.9
weighted mean	19.95	0.26

all five samples (AS1, AS27, AS41, AS46, AS74)

	Age (Ma)	2 sigma error (Ma)
weighted mean	18.89	0.28

Dunkl et al. (2003)

Zircon fission track

	Age (Ma)	2 sigma error (Ma)	Localities in Figure A-1
	16.7	2	w
	17.1	2.6	x
	16.9	1.6	y
	17.5	2	z
weighted mean	17.02	0.98	

Bertrand (pers. comm.)

Zircon fission track

	Age (Ma)	2 sigma error (Ma)	Localities in Figure A-1
	13.1	1	aa
	13.6	2.6	ab
	12.3	1.2	ac
	11.3	4.6	ad
	12.4	2.2	ae
weighted mean	12.76	0.69	

Weighted mean used in Fig. 7 is highlighted with a yellow background

References

Bada G, Grenerczy G, Tóth L, Horváth F, Stein S, Cloetingh S, Windhoffer G, Fodor L, Pinter N, Fejes I (2007) Motion of Adria and ongoing inversion of the Pannonian Basin: seismicity, gps velocities and stress transfer. In: Stein S, Mazzotti S (eds) Continental intraplate earthquakes: science, hazard, and policy issues, Geol Soc Am, Special Paper 425

Beaumont C, Jamiesont RA, Nguyen MH, Lee B (2001) Himalayan tectonics explained by extrusion of a low-viscosity crustal channel coupled to focused surface denudation. Nature 414:738–742

Bechtel A, Reischenbacher D, Sachsenhofer RF, Gratzer R, Lücke A (2007) Paleogeography and paleoecology of the upper Miocene Zillingdorf lignite deposit (Austria). Int J Coal Geol 69:119–143

Becker B (1993) The structural evolution of the Radstsdt thrust system, Eastern Alps, Austria—Kinematics, thrust geometries, strain analysis. Tübinger Geowiss Arbeiten 14:92

Bigi G, Castellarin A, Catalano R, Coli M, Cosentino D, Dal Piaz GV, Lentini F, Parotto M, Patacca E, Praturlon A, Salvini F, Sartori R, Scandone P, Vai G (1989) Synthetic structural kinematic map of Italy, sheets 1 and 2. C.N.R Progetto Finalizzato Geodinamica, SELCA Firenze

Borsi S, DelMoro A, Sassi FP, Zanferrari A, Zirpoli G (1979) On the age of the Vedrette di Ries (Rieserferner) massif and its geodynamic significance. Geol Rundsch 68:41–60. doi:10.1007/BF01821121

Brandner R, Reiter F, Töchterle A (2008) Überblick zu den Ergebnissen der geologischen Vorerkundung für den Brenner-Basistunnel. Geo Alp 5:165–174

Castellarin A, Cantelli L (2000) Neo-Alpine evolution of the Southern Eastern Alps. J Geodyn 30:251–274

Christensen JN, Selverstone J, Rosenfeld JL, DePaolo DJ (1994) Correlation by Rb-Sr geochronology of garnet growth histories from different structural levels within the Tauern Window, Eastern Alps. Contrib Mineral Petrol 118:1–12

Cliff RA, Droop GTR, Rex DC (1985) Alpine metamorphism in the south-east Tauern Window, Austria: 2. rates of heating, cooling and uplift. J Metamorph Geol 3:403–415

Cliff RA, Oberli F, Meier M, Droop GTR (1998) Achieving geological precision in metamorphic geochronology: a Th-Pb age for the syn-metamorphic formation of the Mallnitzermulde Synform, Tauern Window, from individual allanite porphyroblasts. Mineral Mag 62A:337–338

Decker K (1996) Miocene tectonics at the Alpine-Carpathian junction and the evolution of the Vienna Basin. Mitt Ges Geol Bergbaustud Österr 41:33–44

Deutsch A (1984) Young Alpine dykes south of the Tauern Window (Austria): a K-Ar and Sr isotope study. Contrib Mineral Petrol 85:45–57

Dewey JF, Shackleton RM, Chengfa C, Yiyin S (1988) The tectonic evolution of the Tibetan Plateau. Philos Trans R Soc Lond 327:379–413

Doglioni C, Bosellini A (1987) Eoalpine and mesoalpine tectonics in the Southern Alps. Geol Rundschau 76:735–754

Droop GTR (1981) Alpine metamorphism of politic schists in the south-east Tauern Window, Austria. Schweiz Miner Petrogr Mitt 61:237–273

Droop GTR (1985) Alpine metamorphism in the south-east Tauern Window, Austria: 1. P-T variations in space and time. J Metamorph Geol 3:371–402

Dunkl I, Frisch W, Grundmann G (2003) Zircon fission track thermochronology of the southeastern part of the Tauern Window and adjacent Austroalpine margin, Eastern Alps. Eclogae Geol Helv 96:209–217

Eder N, Neubauer N (2000) On the edge of the extruding wedge: neogene kinematics and geomorphology along the southern Niedere Tauern, Eastern Alps. Eclogae Geol Helv 93:81–92

England PC, Thompson AB (1984) Pressure-temperature-time paths of regional metamorphism I. Heat transfer during the evolution of regions of thickened continental crust. J Petrol 25(4):894–928. doi:10.1093/petrology/25.4.894

Exner C (1956) Geologische Karte der Umgebung von Gastein 1:50.000. Wien, Geol BA

Exner C (1962a) Geologische Karte der Sonnblickgruppe 1:50.000. Wien, Geol BA

Exner C (1962b) Sonnblicklammele und Mölltalline. JB Geol BA 105:256–273

Exner C (1962c) Die Perm-Trias-Mulde des Gödnachgrabend an der Störungslinie von Zwischenbergen (Kreuzeckgruppe, östlich Lienz). Verh Geol BA 1962:24–27

Exner C (1964) Erläuterungen zur Geologischen Karte der Sonnblickgruppe. Wien, Geol BA

Exner C (1980) Geologie der Hohen Tauern bei Gmünd in Kärnten. JB Geol BA 123:343–410

Exner C (1983) Geologische Karte der Hafnergruppe 1:25.000 mit Erläuterungen. Mitt Ges Geol Bergbaustud Österr 29:41–74

Exner C (1989) Geologie des mittleren Lungaus. Jb Geol BA 132:7–103

Fodor L, Csontos L, Bada G, Györfi I, Benkovics L (1999) Tertiary evolution of the Pannonian Basin system and neighboring orogens: a new synthesis of palaostress data. In: Durand B, Jolivet L, Horváth F, Seranne M (eds) The Mediterranean Basins: tertiary extension within the Alpine Orogen. Geol Soc Spec Publ 156:295–334

Foeken JPT, Persano C, Stuart FM, ter Voorde M (2007) Role of topography in isotherm perturbation: Apatite (U-Th)/He and fission track results from the Malta tunnel, Tauern Window, Austria. Tectonics 26. doi:10.10129/2006TC002049

Foster DA, Gleadow AJW, Noble WP (1996) Sphene and zircon fission track closure temperature revisited: Empirical calibration from $^{40}Ar/^{39}Ar$ diffusion studies of K—feldspar and biotite. In: Int workshop on fission-track dating, Gent, Abstracts 37

Frank W (1965) Tektonische Gliederung der Glockner und Granatspitzgruppe. Dissertation, University Wien, Wien

Frisch W, Kuhlemann J, Dunkl I, Brügel A (1998) Palinspastic reconstruction and topographic evolution of the Eastern Alps during late Tertiary tectonic extrusion. Tectonophysics 297:1–15

Frisch W, Dunkl I, Kuhlemann J (2000) Post-collisional orogen-parallel large-scale extension in the Eastern Alps. Tectonophysics 327:239–265

Froitzheim N, Plasienka D, Schuster R (2008) Alpine tectonics of the Alps and western Carpathians. In: McCann T (ed) The geology of Central Europe, vol 2, Mesozoic and cenozoic. Geol Soci Lond 1141–1232

Fügenschuh B, Seward D, Mancktelow NS (1997) Exhumation in a convergent orogen: the western Tauern Window. Terra Nova 9:213–217

Fügenschuh B, Mancktelow NS, Schmid SM (2012) Comment on Rosenberg and Garcia: estimating displacement along the Brenner Fault and orogen-parallel extension in the Eastern Alps, Int J Earth Sci (Geol Rundsch) (2011) 100:1129–1145. Int J Earth Sci 101:1451–1455. doi:10.1007/s00531-011-0725-4

Genser J, Neubauer F (1989) Low angle normal faults at the eastern margin of the Tauern window (Eastern Alps). Mitt Österr Geol Gesell 81:233–243

Glodny J, Ring U, Kühn A (2008) Coeval high-pressure metamorphism, thrusting, strike-slip, and extensional shearing in the Tauern Window, Eastern Alps. Tectonics 27(4): TC4004. doi:10.1029/2007TC002193

Gradstein F, Ogg J, Smith AG (2004) A geologic time scale. Cambridge University Press, Cambridge, p 589

Grenerczy G, Sella G, Stein S, Kenyeres A (2005) Tectonic implications of the GPS velocity field in the northern Adriatic region. Geophy Res Lett 32:L16311. doi:10.1029/2005GL022947

Grundmann G, Morteani M (1985) The young uplift and the thermal history of the central Eastern Alps (Austria, Italy). Evidence from apatite fission track ages. JB Geol BA 128:197–216

Handy MR, Oberhänsli R (2004) Metamorphic structure of the Alps, age map of the metamorphic structure of the Alps—tectonic interpretation and outstanding problems. In: Oberhänsli R (ed) Explanatory notes to the map: metamorphic structure of the Alps. Mitt Österr Mineral Ges 149:201–226

Handy MR, Franz L, Heller F, Janott B, Zurbriggen R (1999) Multistage accretion and exhumation of the continental crust (Ivrea crustal section, Italy and Switzerland). Tectonics 18(6):1154–1177

Handy MR, Babist J, Rosenberg CL, Wagner R, Konrad M (2005) Decoupling and is relation to strain partitioning in continental lithosphere—insight from the Periadriatic fault system (European Alps). In: Gapais D, Brun JP, Cobbold PR (eds) Deformation mechanism, rheology and tectonics. Geol Soc Lond Spec Publ 243:249–276

Handy MR, Schmid SM, Bousquet R, Kissling E, Bernoulli D (2010) Reconciling plate—tectonic reconstruction of Alpine Tethys with the geological-geophysical record of spreading and subduction in the Alps. Earth Sci Rev 102:121–158

Harris TM (1981) Diffusion of ^{40}Ar in hornblende. Contrib Mineral Petrol 78:324–331

Harrison MT, Célérier J, Aikman AB, Hermann J, Heizler MT (2009) Diffusion of ^{40}Ar in muscovite. Geochemica et Cosmochimica Acta 73:1039–1051

Heinisch H, Schmidt K (1984) Zur Geologie des Thurntaler Quarzphyllits und des Altkristallind südlich des Tauernfensters (Ostalpen, Südtirol). Geol Rundschau 73:113–129

Hoinkes G, Koller F, Rantitsch G, Dachs E, Hock V, Neubauer F, Schuster R (1999) Alpine metamorphism of the Eastern Alps. Schweiz Mineral Petro Mitt 79:155–181

Hölzel M, Decker K, Zámolyi A, Strauss P, Wagreich M (2010) Lower Miocene structural evolution of the central Vienna Basin (Austria). Marine Pet Geol 27:666–681

Hoke L (1990) The Altkristallin of the Kreuzeck Mountains, SE Tauern Window, Eastern Alps—basement crust in a convergent plate boundary zone. JB Geol BA 133:5–87

Horváth F (1993) Towards a mechanical model for the formation of the Pannonian basin. Tectonophysics 226:333–357

Horváth F, Bada G, Szafian P, Tari G, Adam A, Cloetingh S (2006) Formation and deformation of the Pannonian Basin: constraints from observational data. Geol Soc Lond Memoris 32:191–206. doi:10.1144/GSL.MEM.2006.032.01.11

Inger S, Cliff RA (1994) Timing of metamorphism in the Tauern Window, Eastern Alps: Rb-Sr ages and fabric formation. J Metamorph Geol 12:695–707

Jäger E, Niggli E, Wenk E (1967) Rb-Sr Altersbestimmungen an Glimmern der Zentralalpen. Beitr Geol Karte Schweiz 134:67

Johnson MRW (2002) Shortening budgets and the role of continental subduction during the India-Asia collision. Earth Sci Rev 59:101–123

Kissling E, Schmid SM, Lippitsch R, Ansorge J, Fügenschuh B (2006) Lithosphere structure and tectonic evolution of the Alpine arc: new evidence from high-resolution teleseismic tomography. In: Gee DG, Stephenson RA (eds) European lithosphere dynamics. European Lithosphere Dynamics, Geological Society of London, Memoirs 32:129–145

Kleinschrodt R (1987) Quarzkorngefügeanalyse im Altkristallin südlich des westlichen Tauernfensters (Südtirol/Italien). Erlanger Geol Abh 114:1–82

Kurz W, Neubauer F (1996) Deformation partitioning during updoming of the Sonnblick area in the Tauern Window (Eastern Alps, Austria). J Struct Geol 18(11):1327–1343

Kurz W, Neubauer F, Genser J, Dachs E (1998) Alpine geodynamic evolution of passive and active continental margins sequences in the Tauern Window (Eastern Alps, Austria, Italy): a review. Geol Rundschau 87:225–242

Kurz W, Handler R, Bertoldi C (2008) Tracing the exhumation of the Eclogite Zone (Tauern Window, Eastern Alps) by 40Ar/39Ar dating of white mica in eclogites. Swiss J Geosci 101:191–206. doi:10.1007/s00015-008-1281-1

Kurz W, Wölfler A, Rabitsch R, Genser J (2011) Polyphase movement on the Lavanttal Fault Zone (Eastern Alps): reconciling the evidence from different geochronological indicators. Swiss J Geosci 104:323–343

Lammerer B, Weger M (1998) Footwall uplift in an orogenic wedge: the Tauern Window in the Eastern Alps of Europe. Tectonophysics 285:213–230

Laubscher HPV (1988) The arcs of the Western Alps and the North Apennines: an updated view. Tectonophysics 146(10):67–78

Lenkey L (1999) Geothermics of the Pannonian Basis and its bearing on the tectonics of Basin evolution. Dissertation, Vrije Universiteit, Amsterdam

Linzer HG, Decker K, Peresson H, Dell'Mour R, Frisch W (2002) Balancing orogenic float of the Eastern Alps. Tectonophysics 354:211–237

Lippitsch R, Kissling E, Ansorge J (2003) Upper mantle structure beneath the Alpine orogen from high-resolution teleseismic tomography. J Geoph R 108(B8):2376. doi:10.1029/2002JB002016

Luciani V, Silvestrini A (1996) Planktonic foraminiferal biostratigraphy and paleoclimatology of the Oligocene/Miocene transition from the Monte Brione Formation (northern Italy, Lake Garda). Mem Sci Geol 48:155–169

Luth SW, Willingshofer E (2008) Mapping of the post-collisional cooling history of the Eastern Alps. Swiss J Geosci 101(1):207–223

Means WD (1989) Stretching faults. Geology 17:893–896

Means WD (1990) One-dimensional kinematics of stretching faults. J Struct Geol 12(2):267–272

Mitterbauer U, Behm M, Brückl E, Lippitsch R, Guterch A, Keller GR, Koslovskaya E, Rumpfhuber E-M, Šumanovac F (2011) Shape and origin of the East-Alpine slab constrained by the ALPASS teleseismic model. Tectonophysics 510:195–206

Müller W, Prosser G, Mancktelow NS, Villa I, Kelly S, Viola G, Oberli F, Nemes F, Neubauer F (2001) Geochronical constraints on the evolution of the Periadriatic Fault System (Alps). Int J Earth Sci 90:623–653

Nemes F, Neubauer F, Cloetingh S, Genser J (1997) The Klagenfurth Basin in the Eastern Alps: an intra-orogenic decoupled flexural basin. Tectonophysics 282:189–203

Nussbaum C (2000) Neogene tectonics and thermal maturity of sediments of the easternmost southern Alps (Friuli area, Italy). Dissertation, Univ. de Neuchatel, Neuchatel, Switzerland

Ortner H, Stingl V (2003) 5th workshop of Alpine Geological Studies Field Trip Guide E1: Lower Inn valley (southern margin of the Northern Calcareous Alps, TransAlp traverse). Geol Paläont Mitt Innsbruck 26:1–20

Paulissen WE, Luthi SM, Grunert P, Coric S, Harzhauser M (2011) Integrated high-resolution stratigraphy of a Middle to Late Miocene sedimentary sequence in the central part of the Vienna Basin. Geol Carpath 62(2):155–169

Pieri M, Groppi G (1981) Subsurface geological structure of the Po Plain, Italy. Prog Final Geodyn Publ 414:1–13

Piller WE, Harzhauser M, Mandic O (2007) Miocene Central Paratethys stratigraphy—current status and future directions. Stratigraphy 4:151–168

Plan L, Grasemann B, Spötl C, Decker K, Boch R, Kramers J (2010) Neotectonic extrusion of the Eastern Alps: constraints from U/Th dating of tectonically damaged speleothems. Geology 38:483–486

Polinski RK, Eisbacher GH (1992) Deformation partitioning during polyphase oblique convergence in the Karawanken Mountains, southeastern Alps. J Struct Geol 14(10):1203–1213

Pomella H, Klötzli U, Scholger R, Stipp M, Fügenschuh B (2011) The Northern Giudicarie and the Meran-Mauls fault (Alps, Northern Italy) in the light of new paleomagnetic and geochronical data from boudinaged Eo-Oligocene tonalites. Int J Earth Sci 100:1827–1850. doi:10.1007/s00531-010-0612-4

Pomella H, Stipp M, Fügenschuh B (2012) Thermochronological record of thrusting and strike-slip faulting along the Giudicarie fault system (Alps, Northern Italy). Tectonophysics 579:118–130

Praus O, Pecova J, Petr V, Babuska V, Plomerova J (1990) Magnetotelluric and seismological determination of lithosphere-asthenosphere transition in Central Europe. Phys Earth Planet Inter 60:212–218

Purdy JW, Jäger E (1976) K-Ar ages on rock-forming minerals from the Central Alps. Mem Ist Geol Mineral Univ Padova 30:33

Ratschbacher L, Neubauer F, Schmid SM, Neugebauer J (1989) Extension in compressional orogenic belts: the Eastern Alps. Geology 17:404–407

Ratschbacher L, Merle O, Davy P, Cobbold P (1991a) Lateral extrusion in the eastern Alps, part 1: boundary conditions and experiments scaled for gravity. Tectonics 10:245–256

Ratschbacher L, Frisch W, Linzer HG, Merle O (1991b) Lateral Extrusion in the Eastern Alps, part 2: structural analysis. Tectonics 10(2):257–271

Ratschbacher L, Dingeldey C, Miller C, Hacker BR, McWilliams MO (2004) Formation, subduction, and exhumation of Penninic oceanic crust in the Eastern Alps: time constraints from 40Ar/39Ar geochronology. Tectonophysics 394:155–170

Reinecker J (2000) Stress and deformation: Miocene to present-day tectonics in the Eastern Alps. Tübinger Geowiss Arb Ser A 55:128

Reinecker J, Lenhardt WA (1999) Present-day field and deformation in eastern Austria. Int J Earth Sci 88:532–550

Reischenbacher D, Rifelj H, Sachsenhofer RF, Jelen M, Ćorić S, Gross M, Teichenbacher B (2007) Early Badenian paleoenvironment in the Lavanttal Basin (Mühldorf Formation; Austria): evidence from geochemistry and paleontology. Austrian J Earth Sci 100:202–229

Reiter F, Lenhardt WA, Brandner R (2005) Indications for activity of the Brenner Normal Fault Zone (Tyrol, Austria) from seismological and GPS data. Austrian J Earth Sci 97:16–23

Riedmüller G, Schwaighofer B (1970) Mineralumwandlungen in Myloniten der Oschenikseestörung (Kärnten, Österreich). Mitt Ges Geol Bergbaus Österr 19:315–328

Riedmüller G, Schwaighofer B (1971) Elektronenoptische Untersuchungen von Kaoliniten aus Myloniten der Oschenikseestörung (Kärnten, Österreich). Carinthia II SH 28:253–258

Rosenberg CL, Garcia S (2011) Estimating displacement along the Brenner Fault and orogen-parallel extension in the Eastern Alps. Int J Earth Sci 100:1129–1145

Rosenberg CL, Schneider S (2008) The western termination of the SEMP Fault (eastern Alps) and is bearing on the exhumation of the Tauern Window. Geol Soc Lond Spec Publ 298:197–218

Rosenberg CL, Brun JP, Gapais D (2004) An indentation model of the Eastern Alps and the origin of the Tauern Window. Geology 32:997–1000

Rosenberg CL, Brun JP, Cagnard F, Gapais D (2007) Oblique indentation in the Eastern Alps: insights from laboratory experiments. Tectonics 26. doi:10.1029/2006TC0011960

Royden LH, Burchfield BC (1989) Are systematic variations in thrust belt style related to plate boundary processes? (The western Alps versus the Carparthians). Tectonics 8:51–61

Royden LH, Horváth F, Burchfield BC (1982) Transform faulting, extension and subsidence in the Carpathian Pannonian region. Geol Soc Am Bull 73:717–725

Royden LH, Burchfield BC, King RW, Wang E (1997) Surface deformation and lower crustal flow in Eastern Tibet. Science 276:788–790. doi:10.1126/science.276.5313.788

Ruppel C, Royden L, Hodges KV (1988) Thermal modeling of extensional tectonics: application to pressure-temperature-time histories of metamorphic rocks. Tectonics 7(5):947–957

Sachsenhofer RF, Lankreijer A, Cloetingh S, Ebner F (1997) Subsidence analysis and quantitative basin modeling in the Styrian Basin (Pannonian Basin System, Austria). Tectonophysics 272:175–196

Sachsenhofer RF, Kogler A, Polesny H, Strauss P, Wagreich M (2000) The Neogene Fohnsdorf Basin: basin formation and basin inversion during lateral extrusion in the Eastern Alps (Austria). Geol Rundschau 89:415–430

Sander B (1911) Geologische Studien am Westende der hohen Tauern. Bericht—Denkschrift d kais Akad D Wiss Wien 83:257–319

Scharf A (2013) Lateral extrusion and exhumation of orogenic crust during indentation by rigid Adriatic continental lithosphere–tectonic evolution of the eastern Tauern Window (Eastern Alps, Austria). Dissertation Freie Universität Berlin

Schmid SM, Froitzheim N (1993) Oblique slip and block rotation along the Engadine line. Eclogae Geol Helv 86(2):569–593

Schmid SM, Aebli HR, Heller F, Zingg A (1989) The role of the Periadriatic Line in the tectonic evolution of the Alps. Geol Soc Lond Spec Publ 45:153–171

Schmid SM, Pfiffner OA, Froitzheim N, Schönborn G, Kissling E (1996) Geophysical-geological transect and tectonic evolution of the Swiss-Italian Alps. Tectonics 15:1036–1064. doi:10.1029/96TC00433

Schmid SM, Fügenschuh B, Kissling E, Schuster R (2004) Tectonic Map and overall architecture of the Alpine orogen. Eclogea Geolo Helve 97(1):93–117

Schmid SM, Bernoulli D, Fügenschuh B, Matenco L, Schefer S, Schuster R, Tischler M, Ustaszewski K (2008) The Alpine-Carpathian-Dinaridic orogenic system: correlation and evolution of tectonic units. Swiss J Geosci 101:139–183

Schmid SM, Scharf A, Handy MR, Rosenberg CL (in press) The Tauern Window (Eastern Alps. Austria): a new tectonic map, with cross-sections and a tectonometamorphic synthesis. Swiss J Geosci

Schneider S, Hammerschmidt K, Rosenberg CL (in press) Dating the life-time of ductile shear zones: age constraints from $^{40}Ar/^{39}Ar$ in situ analyses. Earth Planet Sci Lett

Schönborn G (1992) Alpine tectonics and kinematic models of the Central Southern Alps. Mem Sci Geol Univ Padova 44:229–393

Schönborn G (1999) Balancing cross sections with kinematic constraints: the Dolomites (northern Italy). Tectonics 18(3):527–545

Schumacher ME, Schönborn G, Bernoulli D, Laubscher HP (1997) Rifting and collision in the Southern Alps. In: Pfiffner OA, Lehner P, Heitzmann P, Müller St, Steck A (eds) Deep structure of the Alps: results of NFP20. Birkhäuserverlag Basel, Switzerland

Sciunnach D, Scardia G, Tremolada F, Silva IP (2010) The Monte Orfano Conglomerate revisited: stratigraphic constraints on Cenozoic tectonic uplift of the Southern Alps (Lombardy, northern Italy). Int J Earth Sci 99:1335–1355. doi:10.1007/s00531-009-0452-2

Selverstone J (1988) Evidence for east-west crustal extension in the Eastern Alps: implications for the unroofing history of the Tauern Window. Tectonics 7:87–105

Selverstone J (2005) Are the Alps collapsing? Annu Rev Earth Planet Sci 33:113–132

Selverstone J, Axen GJ, Bartley JM (1995) Fluid inclusion constraints on the kinematics of footwall uplift beneath the Brenner Line normal fault, eastern Alps. Tectonics 14:264–278

Senftl E, Exner Ch (1973) Rezente Hebung der Hohen Tauern und geologische interpretation. Verh Geol BA 2:209–234

Siivola J, Schmid R (2007) Recommendations by the IUGS Subcommission on the systematics of metamorphic rocks: list of mineral abbreviations. Web version 01.02.07. IUGS Commission on the Systematics in Petrology

Slejko D, Carulli GB, Nicolich R, Rebez A, Zanferrari A, Cavallin A, Doglioni C, Carraro F, Castaldini D, Illiceto V, Semenza E, Zanolla C (1989) Seismotectonics of the Eastern Southern-Alps: a review. Boll Geof Teor Appl 31(122):109–136

Steininger FF, Wessely G (2000) From the Tethyan Ocean to the Paratethys Sea: Oligocene to Neogene stratigraphy, Paleogeography and Paleobiography of the circum-Mediterranean region and the Oligocene to Neogene Basin evolution in Austria. Mitt Österr Geo Ges 92:95–116

Stipp M, Stünitz H, Heilbronner R, Schmid SM (2002) The eastern Tonale fault zone: a natural laboratory for crystal plastic deformation of quartz over a temperature range from 250 to 700 °C. J Struct Geol 24:1861–1884

Stipp M, Fügenschuh B, Gromet LP, Stünitz H, Schmid SM (2004) Contemporaneous plutonism and strike-slip faulting: a case study from the Tonale fault zone north of the Adamello pluton (Italian Alps). Tectonics 23. doi:10.1029/2003TC001515

Strauss P, Wagreich M, Decker K, Sachsenhofer RF (2001) Tectonics and sedimentation in the Fohnsdorf-Seckau Basin (Miocene, Austria): from a pull-apart basin to a half-graben. Int J Earth Sci 90:549–559. doi:10.1007/s005310000180

Tapponnier P, Peltzer G, Armijo R (1986) On the mechanics of the collision between India and Asia. Geol Soc Lond Spec Publ 19:113–157

Töchterle A, Brandner R, Reiter F (2011) Strain partitioning on major fault zones in the northwestern Tauern window—insights from the investigations of the Brenner base tunnel. Austrian J Earth Sci 104:15–35

Tomljenovic B, Csontos L (2001) Neogene-Quarternary structures in the border zone between Alps, Dinarides and Pannonian Basin (Hrvatsko zagorje and Karlovac Basin, Croatia). Int J Earth Sci 90:560–578

Ustaszewski K, Schmid SM, Fügenschuh B, Tischler M, Kissling E, Spakman W (2008) A map-view restoration of the Alpine-Carpathian-Dinaridic system for the Early Miocene. Swiss J Geosci 101:273–294. doi:10.1007/s00015-008-1288-7

Venzo S (1940) Studio geotettonico del Trentino meridionale-orientale tra Borgo Valsugana e M. Coppolo. Mem Ist Geol Univ Padova 14:1–86

von Blanckenburg F, Davies JH (1995) Slab break off: a model for syncollisional magmatism and tectonics in the Alps. Tectonics 14:120–131

von Blanckenburg F, Villa IM (1988) Argon retentivity and argon excess in amphiboles from the garbenschists of the Western Tauern Window, Eastern Alps. Contrib Mineral Petrol 100:1–11

von Blanckenburg F, Villa IM, Baur H, Morteani G, Steiger RH (1989) Time calibration of PT-path from the Western Tauern Window, Eastern Alps: the problem of closure temperatures. Contrib Mineral Petrol 101:1–11

Vrabec M, Fodor L (2006) Late Cenozoic tectonics of Slovenia: structural styles at the northeastern corner of the Adriatic microplate. In: Pinter N, Grenerczy G, Weber J, Stein S, Medak D (eds) The Adria microplate: GPS geodesy, tectonics and hazards, vol 61: Nato Scie Series, IV, earth and environmental science. Springer, Dordrecht, pp 151–158

Vrabec M, Preseren PP, Stopar B (2006) GPS study (1996–2002) of active deformation along the Periadriatic fault system in northeastern Slovenia: tectonic model. Geol Carpath 57:57–65

Wagner R, Rosenberg CL, Handy MR, Möbus C, Albertz M (2006) Fracture-driven intrusion and upwelling of a mid-crustal pluton fed from a transpressive shear zone—the Rieserferner Pluton (Eastern Alps). GSA Bull 118:219–237

Waldhauser F, Lippitsch R, Kissling E, Ansorge J (2002) High-resolution teleseismic tomography of upper mantle structure using an a priori three-dimensional crustal model. Geophys J Int 150:403–414

Wiederkehr M, Sudo M, Bousquet R, Berger A, Schmid SM (2009) Alpine orogenic evolution from subduction to collisional thermal overprint: the $^{40}Ar/^{39}Ar$ age constraints from the Valaisan Ocean, Central Alps. Tectonics 28(TC6009):1–28. doi:10.1029/2009TC002496

Wölfler A, Dekant C, Danišik M, Kurz W, Dunkl I, Putiš M, Frisch W (2008) Late stage differential exhumation of crustal blocks in the central Eastern Alps: evidence from fission track and (U-Th)/He thermochronology. Terra Nova 20:378–384

Wölfler A, Kurz W, Danišik M, Rabitsch R (2010) Dating of fault zone activity by apatite fission track and apatite (U-Th)/He thermochronometry: a case study from the Lavanttal fault system (Eastern Alps). Terra Nova 22:274–282

Wölfler A, Kurz W, Fritz H, Stüwe K (2011) Lateral extrusion in the Eastern Alps revisited: Refining the model by thermochronological, sedimentary, and seismic data. Tectonics 30. doi:10.1029/2010TC002782

Wölfler A, Stüwe K, Danišik M, Evans NJ (2012) Low temperature thermochronology in the Eastern Alps: implications for structural and topographic evolution. Tectonophysics 541–543:1–18

Zanchi A, D'Adda P, Zanchetta S, Berra F (2012) Syn-thrust deformation across a transverse zone (central Southern Alps, N. Italy). Swiss J Geosci 105:19–38

Zeilinger G (1997) Das Tamsweger Tertiär: Fazies und Deformation eines intramontanen Beckens und seine regionale geodynamische Bedeutung. Diploma Thesis at University Tübingen